



CFC-11 measurements in China, Nepal, Pakistan, Saudi Arabia and South Korea (1998–2018): Urban, landfill fire and garbage burning sources

Isobel J. Simpson^{A,*} , Barbara Barletta^A, Simone Meinardi^A, Omar Siraj Aburizaiza^B, Peter F. DeCarlo^C, Muhammad Akhyar Farrukh^D , Haider Khwaja^{E,F}, Jinseok Kim^G, Younha Kim^H, Arnico Panday^{I,J}, Azhar Siddique^K, Elizabeth A. Stone^L, Tao Wang^M, Jung-Hun Woo^G, Likun Xue^N, Robert J. Yokelson^O, Jahan Zeb^P and Donald R. Blake^A

Environmental context. The production and consumption of chlorofluorocarbons (CFCs) is regulated under the Montreal Protocol and its amendments, due to their role in stratospheric ozone depletion. Global atmospheric levels of CFC-11 did not decline as rapidly as expected during 2012–2018, in large part due to emissions from eastern China. In order to further clarify global CFC-11 emissions, this work provides a rare set CFC-11 measurements from understudied countries and sources throughout Asia (1998–2018).

For full list of author affiliations and declarations see end of paper

***Correspondence to:**

Isobel J. Simpson
 Department of Chemistry, University of California–Irvine (UCI), Irvine, CA, USA
 Email: isimpson@uci.edu

Handling Editor:

Ying Chen

Received: 5 October 2021

Accepted: 13 February 2022

Published: 12 April 2022

Cite this:

Simpson IJ *et al.* (2021)
Environmental Chemistry
 18(8), 370–392. doi:[10.1071/EN21139](https://doi.org/10.1071/EN21139)

© 2021 The Author(s) (or their employer(s)). Published by CSIRO Publishing.

This is an open access article distributed under the Creative Commons Attribution-NonCommercial-NoDerivatives 4.0 International License ([CC BY-NC-ND](https://creativecommons.org/licenses/by-nc-nd/4.0/))

OPEN ACCESS

ABSTRACT

Trichlorofluoromethane (CFC-11) is an ozone-depleting substance whose production and consumption are regulated under the Montreal Protocol. Global atmospheric CFC-11 levels declined less quickly than expected during 2012–2018, largely because of ongoing emissions from eastern Asia. Satellite measurements suggest additional CFC-11 hotspots in the Arabian Peninsula and north India/Nepal. Here we present CFC-11 levels measured in dozens of Asian cities during 1998–2018, including China and Pakistan before the 2010 phaseout of CFC-11, and China, Nepal, Pakistan, Saudi Arabia and South Korea after the phaseout. Surface measurements of CFCs in Nepal, Pakistan and Saudi Arabia are very rare, and these surveys provide important observational constraints from understudied regions. During pre-phaseout campaigns, higher CFC-11 levels were measured in Beijing than Karachi, despite much higher overall volatile organic compound (VOC) levels in Karachi. During post-phaseout campaigns, average CFC-11 levels were higher in inland Shandong Province and Seoul (1.11–1.23× background) than in western Saudi Arabia, Lahore and Kathmandu (1.02–1.11× background), despite higher levels of other VOCs in the latter regions. While China is known to emit excess CFC-11, elevated CFC-11 levels in Seoul, especially during stagnant meteorological conditions, suggest local emissions in 2015–2016. Rough emission estimates suggest that South Korea is likely a relatively minor global source of excess CFC-11. Hotspot CFC-11 levels were measured from a landfill fire in Mecca (average of 1.8× background) and from garbage burning in Nepal (1.5× background). Because garbage burning and open burning in dumps are common practices, further investigation of CFC-11 emissions at dumps and landfills worldwide is encouraged to determine their global impact.

Keywords: Asia, CFC-11, chlorofluorocarbons, emissions, landfill fire, garbage burning, Montreal Protocol, ozone depletion, surface measurements.

Introduction

Trichlorofluoromethane (CCl₃F, CFC-11) is an ozone-depleting substance and greenhouse gas that was used primarily as a foam-blowing agent, before its regulation under the 1987 Montreal Protocol and its amendments. Following the discovery that CFCs deplete stratospheric ozone, the production and consumption of CFC-11 was restricted in developed countries by 1996 with a global phaseout by 2010, leading to a decline in global CFC-11

levels (Carpenter and Reimann 2014). However, using global data from the National Oceanic and Atmospheric Administration (NOAA), Montzka *et al.* (2018) reported that the rate of decline in global CFC-11 concentrations began slowing in 2013, caused by an estimated $13 \pm 5 \text{ Gg year}^{-1}$ ($25 \pm 13\%$) increase in CFC-11 emissions since 2012. The increase was consistent with unreported new production, as opposed to a substantial increase in emissions from existing banks such as CFC-11 in closed-cell foams (Montzka *et al.* 2018). Based on measurements from both NOAA and the Advanced Global Atmospheric Gases Experiment (AGAGE), global CFC-11 emissions during 2014–2016 were estimated to be 10 Gg year^{-1} higher than emissions during 2002–2012 (Engel and Rigby 2018). AGAGE measurements coupled with chemical transport modeling were further used to estimate that CFC-11 emissions from eastern mainland China, primarily Shandong and Hebei provinces, were $7.0 \pm 3.0 \text{ Gg year}^{-1}$ higher in 2014–2017 than 2008–2012 (Rigby *et al.* 2019). Together these calculations suggested that a large fraction ($60 \pm 40\%$) of the unreported CFC-11 production could be attributed to eastern China (Park *et al.* 2021), although a substantial portion of the unreported production remained unaccounted for. Using near-global Atmospheric Infrared Sounder (AIRS) retrievals from NASA's Aqua satellite, Chen *et al.* (2020) found that CFC-11 trends during 2003–2018 were less negative over the Shandong Peninsula, the Arabian Peninsula and north India and Nepal compared to 2003–2012, suggesting relatively elevated emissions in recent years in these regions. Recent analysis shows a renewed decline in CFC-11 emissions from 2018 to 2019 of $18 \pm 6 \text{ Gg year}^{-1}$, with 2019 emissions similar to the 2008–2012 mean (Montzka *et al.* 2021). The emission reductions likely resulted from increased enforcement taken in China and elsewhere after 2017 (Montzka *et al.* 2021; Park *et al.* 2021).

In order to better understand CFC-11 sources and emission changes in different regions of Asia, we present CFC-11 measurements from ground-based and airborne field studies in five Asian countries from 1998 to 2018. Pre-phaseout CFC-11 measurements from ground-based campaigns in China and Pakistan are presented for perspective (1998–2008). The global phaseout of CFCs was staggered, with a schedule of 50% reduction by January 1, 2005, 85% by January 1, 2007 and 100% reduction by January 1, 2010 for Article 5 countries (Technology and Economic Assessment Panel (TEAP) 2021). Therefore, some of the pre-phaseout studies overlap this period of reduction. Post-phaseout measurements include ground-based sampling in China, Nepal, Pakistan, Saudi Arabia and South Korea (2012–2018) and airborne sampling of South Korea and eastern China (2016). These are the only observational ground-based CFC-11 data that we are aware of for Nepal, Pakistan and Saudi Arabia, and they provide valuable insights into ongoing CFC-11 emission locations or hotspots, as well as locations where CFC-11 emissions are low. In addition, the

observations provide information on co-emitted gases and potential CFC-11 sources. For example, carbon tetrachloride (CCl_4) is a feedstock for CFC-11, and CFC-12 may be co-produced with CFC-11 (Carpenter and Reimann 2014; Harris *et al.* 2019; Park *et al.* 2021). Therefore, the presence or absence of correlating species within hotspot CFC-11 locations are used to investigate CFC-11 sources.

Methods

In cooperation with numerous colleagues, the University of California at Irvine (UCI) has performed urban air sampling campaigns in more than 80 cities since the 1990s, including more than 50 cities in Asia (e.g. Blake and Rowland 1995; Barletta *et al.* 2002, 2006, 2017; Simpson *et al.* 2014, 2020; Stockwell *et al.* 2016; Kim *et al.* 2018b; Islam *et al.* 2020). These datasets have been used to characterise volatile organic compound (VOC) emissions, sources and reactivity in different urban areas, including understudied countries such as Nepal, Pakistan and Saudi Arabia. Below we briefly describe the ground-based and airborne air sampling campaigns in Asia, which are shown in Fig. 1 and summarised in Table 1.

Canister-based air sampling

All campaigns used canister-based whole air sampling (WAS) followed by laboratory analysis at UCI using multi-column gas chromatography. Procedures to prepare the canisters for field use are described in Simpson *et al.* (2020). Air samples were collected into evacuated, electropolished 2 L conditioned stainless steel canisters, each equipped with a Swagelok Nupro metal bellows valve. During ground-based sampling the valve is slightly opened to allow air to enter into the evacuated canister, and the valve is closed once air in the canister reaches ambient pressure, typically after about 30–60 s (Fig. 2). During airborne sampling, a dual-head metal bellows pump was used to draw air from outside the aircraft, via a $\frac{1}{4}$ " stainless steel inlet tube to an air sampling manifold and into a canister (Simpson *et al.* 2020). Each canister was opened until it was pressurised to 40 psi (275 kPa) and then the valve was closed. The typical sampling duration during airborne sampling was 40 s.

Concentrations in urban areas are influenced by a number of factors including distance from sources, local meteorology, time of day and so forth. UCI's urban sampling campaigns have been designed to minimise potential bias from these effects as much as possible. Samples are collected at multiple locations within each city and at different times of the day over multiple days. Samples are typically collected in open spaces away from local source influences, unless roadside and industrial zones are being targeted. Overall, the campaigns are intended to be a representative snapshot of the urban environment, with minimal influence from immediate emission sources.

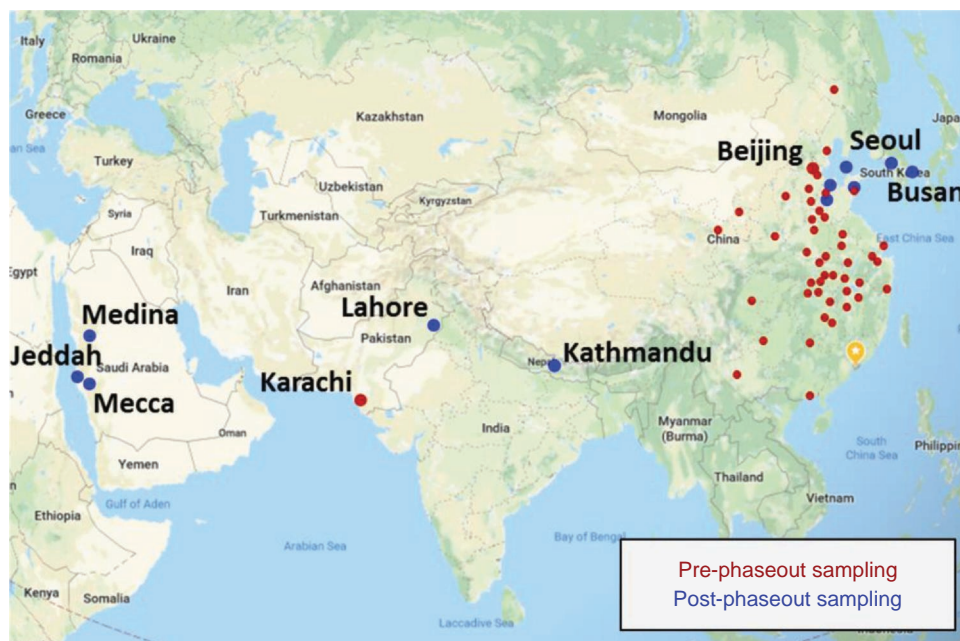


Fig. 1. Locations of urban air sampling campaigns performed in Asia by UCI and colleagues during 1998–2018. Red = campaigns before the 2010 global phaseout of CFC-11; blue = campaigns after the phaseout. Smaller red dots indicate cities sampled during a 45-city study of China.

Pre-phaseout sampling campaigns

Four ground-based air sampling campaigns were carried out during 1998–2008 (two in China and two in Pakistan), before the 2010 phaseout of CFC-11. These campaigns provide context for the range of CFC-11 concentrations that occurred before the regulations took effect. Maps of the sampling locations are presented together with the results in the *Results* section. Sampling coordinates, sampling times and campaign duration are summarised in [Table 1](#).

1) China (2001): 45 cities ($n = 158$)

Air samples were collected in 45 Chinese cities during China's Lunar New Year holidays (January 11 to February 14, 2001), with 2–6 samples collected per city in commercial, residential and urban spaces ([Barletta et al. 2006](#)).

2) China (2008): Beijing Olympics ($n = 332$)

Beijing (population (pop.) of 15 million in 2008) hosted the Summer Olympic Games from August 8 to 24, 2008. Air samples were collected in the Beijing area before, during and after the Olympics (July 10–November 28), including the Beijing city centre ($n = 37$); the Chinese Research Academy of Environmental Sciences (CRAES) about 15 km north of central Beijing ($n = 150$); Heishanzhai, a rural mountainous area 50 km north of Beijing ($n = 108$) and Xicicun, a farmland area 55 km to the south of Beijing ($n = 37$) ([Wang et al. 2010](#)).

3) Pakistan (1998/1999 and 2006): Karachi ($n = 163$)

Karachi (pop. 9.4 million in 1998 and 11.4 million in 2006) is the largest city in Pakistan. Air samples were collected in roadside, urban and industrial areas of Karachi from December 10, 1998 to January 15, 1999 ($n = 80$; [Barletta et al. 2002](#)) and January 14–26, 2006 ($n = 83$).

Post-phaseout sampling campaigns

Multiple ground-based air sampling campaigns were conducted during 2012–2018 in China, Nepal, Pakistan, Saudi Arabia and South Korea. The airborne Korea–United States Air Quality Study (KORUS-AQ) sampled emissions from South Korea and China in spring, 2016. Each campaign is described below. As with the pre-phaseout campaigns, maps of the sampling locations are shown in the *Results* section and sampling details are summarised in [Table 1](#).

1) Pakistan (2012): Lahore ($n = 48$)

Lahore (pop. 9.2 million in 2012) is the capital of Punjab. Air samples were collected throughout Lahore (December 29–31, 2012), including roadside, urban, suburban and industrial sites ([Barletta et al. 2017](#), [Fig. 2a](#)).

2) Saudi Arabia (2012, 2013): Mecca, Medina, Jeddah ($n = 172$)

Three air sampling campaigns were conducted in western Saudi Arabia from 2012 to 2013: October 18 to November 13,

Table 1. Summary of urban studies conducted in Asia by UCI (1998–2018).

Country	City/place	Latitude	Longitude	Year	Sampling dates	Sampling times	Comments	Bkgd locations (count)
Pre-phaseout (before 2010)								
China	45 cities	see text	see text	2001	Jan 11–Feb 14	07:30–20:30	–	OR, CA, S Baja (9)
China	Beijing	39.9°N	116.4°E	2008	Jul 10–Nov 28	07:00–19:00	Olympics	WA, OR, CA (12)
Pakistan	Karachi	24.9°N	67.0°E	1998–1999	Dec 10–Jan 15	around clock	–	S Baja, Kauai, Hawaii (16)
Pakistan	Karachi	24.9°N	67.0°E	2006	Jan 14–31	around clock	–	S Baja, Hawaii (17)
Post-phaseout (after 2010)								
Pakistan	Lahore	31.5°N	74.3°E	2012	Dec 29–31	around clock	–	CA, N Baja (8)
Saudi Arabia	Mecca	21.4°N	39.9°E	2012	Oct 18–Nov 12	11:00–24:00	Hajj	S Baja, Hawaii (8)
Saudi Arabia	Jeddah	21.5°N	39.2°E	2012	Oct 18–Nov 13	10:00–24:00	Hajj	S Baja, Hawaii (8)
Saudi Arabia	Medina	24.5°N	39.6°E	2012	Oct 19–Nov 11	13:00–24:00	Hajj	S Baja, Hawaii (8)
Saudi Arabia	Mecca	21.4°N	39.9°E	2013	Apr 7–12	14:00–02:00	Non-Hajj	S Baja, Hawaii (8)
Saudi Arabia	Mecca landfill	21.4°N	39.9°E	2013	May 26	10:20–10:45	Non-Hajj	S Baja, Hawaii (4)
Saudi Arabia	Jeddah	21.5°N	39.2°E	2013	Apr 8–13	12:00–02:00	Non-Hajj	S Baja, Hawaii (8)
Saudi Arabia	Medina	24.5°N	39.6°E	2013	Apr 11–12	18:00–01:00	Non-Hajj	S Baja, Hawaii (8)
Saudi Arabia	Mecca	21.4°N	39.9°E	2013	Oct 10–19	05:00–21:00	Hajj	S Baja, Hawaii (14)
Saudi Arabia	Jeddah	21.5°N	39.2°E	2013	Oct 18–19	11:00–24:00	Hajj	S Baja, Hawaii (14)
Nepal	Bode	27.7°N	85.3°E	2015	Apr 12–Jun 8	07:00–19:00	NAMaSTE	N Baja, S Baja (9)
Nepal	Kathmandu	27.7°N	85.3°E	2018	Apr 12–20	06:00–22:00	–	N Baja, S Baja (9)
China	Mount Tai	36.2°N	117.1°E	2014	Jun 4–Jul 14	08:00–24:00	Shandong	CA, N Baja (5)
China	Tuoji Island	38.2°N	120.8°E	2014	Dec 11–22	07:00–16:00	Shandong	CA (4)
China	Dongying	37.4°N	118.7°E	2016	Sep (dates n/a)	n/a	Shandong	CA, N Baja (6)
China	Qingdao	36.1°N	120.2°E	2018	Mar 22–Apr 5	10:00–01:00	Shandong	CA, N Baja (8)
China	Yellow Sea	see text	see text	2016	Jun 2–5	08:00–16:00	KORUS-AQ	CA, N Baja (6)
South Korea	Seoul	37.6°N	127.0°E	2015	May 23–Jun 10	09:00–15:00	MAPS-Seoul	CA, N Baja (6)
South Korea	Seoul	37.6°N	127.0°E	2016	May 22–Jun 10	08:00–16:00	KORUS-AQ	CA, N Baja (6)
South Korea	Daesan	36.9°N	126.4°E	2016	May 22–Jun 5	10:00–14:00	KORUS-AQ	CA, N Baja (6)
South Korea	Busan	35.2°N	129.1°E	2016	May 7–Jun 3	08:00–16:00	KORUS-AQ	CA, N Baja (6)

All sampling campaigns were ground-based except KORUS-AQ. n/a = not available. 'around clock' = sampling at specific times around the clock. Background (bkgd) locations: Washington (WA) = 46–47°N, Oregon (OR) = 42–45°N, California (CA) = 36–41°N, North Baja (N Baja) = 29–31°N, South Baja (S Baja) = 22–24°N, Kauai = 22°N, Hawaii = 20°N.

2012 ($n = 77$); April 7–12, 2013 ($n = 54$) and October 15–19, 2013 ($n = 36$) (a landfill fire in Mecca was also sampled; $n = 5$). All campaigns sampled Mecca and Jeddah, and the first two campaigns also sampled Medina (Simpson *et al.* 2014; Barletta *et al.* 2017). The two October campaigns overlapped with the annual Hajj pilgrimage, which brought millions of pilgrims to Mecca and the surrounding region.

1. *Jeddah* (2012, $n = 10$; 2013, $n = 33$). Jeddah (pop. 5.1 million in 2012) is the second-largest city in Saudi Arabia. Air samples were collected primarily in residential districts.
2. *Mecca/Makkah* (2012, $n = 46$; 2013, $n = 46$). Mecca (pop. 2 million in 2012) lies 70 km east of Jeddah. Air samples were collected near the Grand Mosque and in residential and commercial districts. Samples were also



Fig. 2. Canister sampling during selected field campaigns. (a) Kot Lakhpat industrial zone, Lahore, Pakistan (2012); (b) landfill fire, Mecca, Saudi Arabia (2013); (c) roadside garbage burning, Nepal (2015); (d) low-altitude airborne sampling over Seoul, South Korea (2016).

collected at a landfill fire 20 km south of Mecca on May 26, 2013 ($n = 5$; Fig. 2b).

3. *Medina/Madinah* (2012, $n = 21$; 2013, $n = 11$). Medina (pop. 1.2 million in 2012) is home to al-Masjid an-Nabawi, or the Prophet's Mosque, which is a major pilgrimage site. Air samples were collected near the Mosque and in residential districts.

3) Nepal (2015, 2018): Kathmandu/Bode ($n = 50$)

Kathmandu (pop. 1.2 million in 2015 and 1.4 million in 2018) is the capital of Nepal and sits in a bowl-shaped valley that encompasses the districts of Kathmandu, Bhaktapur and Lalitpur (total pop. of over 3 million). Bode is a suburban location in the Bhaktapur District, about 10 km east of central Kathmandu and 4 km east of Kathmandu's airport.

1. *Bode* (2015; $n = 15$). Air samples were collected in Bode during April 16–24 and June 6–8, 2015, as part of the Nepal Ambient Monitoring and Source Testing Experiment (NAMaSTE; Stockwell et al. 2016; Goetz et al. 2018; Islam et al. 2020). Fewer samples than planned were taken ($n = 9$) because the campaign was interrupted by the Gorkha Earthquake on April 25, 2015. A limited number of garbage burning samples were collected in Bode and Kathmandu ($n = 6$), including roadside garbage (Fig. 2c) and mixed household waste (vegetables, cardboard, plastic, etc.).

2. *Kathmandu Valley* (2018; $n = 35$). Air samples were collected around the Kathmandu Valley during April 12–20, 2018 during the pre-monsoon season. Sampling sites included the Ring Road around Kathmandu city, Chandragiri Mountain (2500 m asl, 10 km southwest of Kathmandu) and along the highway to Dhulikhel (30 km east of Kathmandu).

4) China (2014–2018): Shandong province ($n = 199$)

Shandong (pop. 100 million) is a coastal province in northeast China with large coal and oil reserves. In coordination with Shandong University, 199 samples were collected at four sites in Shandong Province from 2014 to 2018.

1. *Mount Tai* (2014; $n = 70$). Mount Tai is located inland in western Shandong province, about 55 km south of the capital Jinan (pop. 8.7 million) and 10 km north of Tai'an (pop. 5.5 million). Mount Tai was sampled from June 4 to July 14, 2014 (Zhao et al. 2022).
2. *Tuoji Island* (2014; $n = 48$). Tuoji Island (pop. < 10 000), a background monitoring site in the Bohai Strait between the Yellow and Bohai Seas (Zhang et al. 2014), was sampled from December 11–22, 2014.
3. *Dongying* (2016; $n = 49$). Dongying (pop. 2.0 million) lies in northern Shandong province and services the Shengli oil field (Zheng et al. 2019). Dongying was sampled in

September 2016, but the exact sampling days and times are not available.

4. *Qingdao (or Tsingtao)* (2018; $n = 32$). Qingdao (pop. 9.0 million) is a coastal city in eastern Shandong province that has seen rapid economic development. Qingdao was sampled from March 22 to April 5, 2018, and was also sampled during the 45-city study in 2001 (see *China (2001): 45 cities* section above).

5) South Korea (2015, 2016): MAPS-Seoul, KORUS-AQ ($n = 2577$)

Seoul (pop. 10 million) is the capital of South Korea. The greater Seoul Metropolitan Area (SMA) has a population of about 25 million people, or roughly half the population of South Korea.

1. *Seoul* (2015; $n = 23$). Ground-based samples were collected in Seoul at the Korea Institute for Science and Technology (KIST) from May 23 to June 10, 2015 (1 year before KORUS-AQ) as part of the Megacity Air Pollution Study (MAPS)-Seoul (Kim *et al.* 2018a).
2. *KORUS-AQ* (2016; $n = 2554$). Air from both China and South Korea was sampled during the airborne KORUS-AQ campaign (Simpson *et al.* 2020), which deployed 20 research flights from May 2 to June 10, 2016 during both stagnant and dynamic meteorological conditions (Peterson *et al.* 2019; Crawford *et al.* 2021). Stagnant conditions encompass stagnation under a persistent anticyclone (May 17–22) and a blocking pattern (June 1–7). Dynamic conditions include dynamic meteorology (May 1–16) and a combination of dynamic meteorology, low-level transport, and haze development (May 25–31). Sustained long-range transport of pollution was limited to the second dynamic period, and most of the pollution sampled during KORUS-AQ originated from local Korean sources (Peterson *et al.* 2019). In the text below, ‘low-altitude’ denotes altitudes < 500 m.

2a. *Seoul, South Korea* ($n = 177$). Low-altitude air samples were collected over Seoul based on low-altitude passes over Olympic Park (~ 300 m) that transitioned to missed approaches (< 30 m) over the Seoul Air Base, about 15 km southeast of central Seoul (Fig. 2d). The samples were collected during both stagnant and dynamic conditions.

2b. *Daesan, South Korea* ($n = 41$). The Daesan petrochemical complex is a major industrial facility about 80 km southwest of Seoul (Fried *et al.* 2020). Low-altitude samples were collected downwind of Daesan during June 2–5, 2016 during stagnant conditions.

2c. *Busan, South Korea* ($n = 32$). Located in southeast Korea, Busan (pop. 3.4 million in 2016) is the busiest port and second-most populated city in South Korea. Low-altitude samples were collected in the Busan

region from May 7 to June 3, 2016 during both stagnant and dynamic conditions.

2d. *Outflow from China* ($n = 66$). Air originating from China was sampled at low altitude over the Yellow Sea (upwind of Korea) during May 4–12 and May 25–31, 2016 during dynamic transport conditions, when transboundary transport from China was at a maximum (Crawford *et al.* 2021). Back-trajectories and model simulations show that the air masses originated from northeast China, including Shandong and Hebei provinces (Simpson *et al.* 2020).

Laboratory analysis of whole air samples

All air samples were analysed at UCI for CFC-11 and ~ 80 additional VOCs using multi-column gas chromatography (GC) with flame ionisation detection (FID), electron capture detection (ECD) and a mass spectrometer detector (MSD) operating in selected ion monitoring (SIM) mode. For ground-based campaigns, $217\text{--}790\text{ cm}^3$ of sample air was drawn from each canister for analysis, depending on the campaign and the amount of pollution in the air samples. For KORUS-AQ, which had pressurised air samples, 2410 cm^3 of sample air was injected into the analytical system. Multiple working standards matching the different volumes of injected air were used.

The UCI analytical system is described in Colman *et al.* (2001) and Simpson *et al.* (2020). After injection, sample air is cryogenically pre-concentrated in a loop filled with glass beads and immersed in liquid nitrogen. Target compounds (including CFC-11) are trapped inside the loop and re-volatilised when the loop is immersed into hot water. A helium flow carries the sample air to a splitter manifold, which directs the air into five streams, each to a different column/detector combination housed in one of three GCs (HP 6890). CFC-11 is measured using Restek-1701/ECD and Restek-1701+DB-5/ECD. (Although CFC-11 can also be measured with DB-5ms/MSD, the measurements are less precise and are not used.) If the percent standard deviation of the CFC-11 standard measurements is similar for each ECD, their results are averaged for a given sample. If not, the ECD with the better precision is used. CFC-11 was measured using Restek-1701/ECD during the 2012 Lahore study, the 2015 Nepal study and the 2015 and 2016 Korea studies. The other studies use CFC-11 averages from both ECDs. CFC-11 linearity tests were performed for both ECD column/detector combinations, with $r^2 = 0.998$ for the Restek-1701+DB-5 and $r^2 = 0.9995$ for the Restek-1701 in the volume range from 270 to 2440 cm^3 .

CFC-11 is calibrated using in-house standards, which represents a UCI scale. The first UCI CFC-11 standard was made in 1978 and a second was made in 1985 (mixing ratio of 215 pptv). The standards were made using a four-step static dilution process in zero air (Tyler 1983; Gilpin 1991). Pure research-grade, liquid CFC-11 from the Matheson Gas

Company was diluted to parts per hundred (pphv) to parts per million (ppmv) to parts per billion (ppbv) to parts per trillion (pptv) on a glass dilution line. The final standard dilution resulted in concentrations close to typical atmospheric values. The accuracy of the four-step static dilution was substantiated in collaboration with Ray Weiss (Scripps Institute of Oceanography) using an independent standard dilution method based on a known mixture of N₂O, CFC-11, CFC-12 and CFC-113. The uncertainty of the standards prepared from the four-step dilution was determined to be $\pm 1.6\%$.

The 1985 CFC-11 standard was housed in a pontoon together with a C₂–C₆ hydrocarbon mix, and this was the primary CFC-11 standard until 1996. Subsequent CFC-11 standards were made, put into pressurised pontoons and compared to the 1985 pontoon. In this way, UCI has used several pontoons that were originally referenced to the 1985 pontoon, and daughters of these subsequent pontoons (granddaughters of the 1985 pontoon) are still used today. The precision of the UCI CFC-11 measurements is 1% and the accuracy is conservatively estimated to be $\pm 3\%$. UCI participated in the International Halocarbons in Air Comparison Experiment (IHALACE), which showed a 1.1% difference between the volume-based UCI scale and the mass-based NOAA CFC-11 scale, or about 2.5 pptv (Hall et al. 2014).

Several other VOCs are reported in this manuscript, in addition to CFC-11. Hydrochlorofluorocarbons (HCFCs), 1,2-dichloroethane (1,2-DCE) and carbonyl sulfide (OCS) were measured using MSD; CFC-12, CFC-113 and CFC-114 (sum of CFC-114 and CFC-114a) were measured using ECD; and alkanes, alkenes and aromatics were measured using FID. Additional analytical details are given in Simpson et al. (2020). The combustion tracer carbon monoxide (CO) was also used in this work. During ground-based missions, CO was measured by UCI using GC/FID (HP 5890) and a 3 mm ID, 5 m molecular sieve column, with a 2% precision and 5% accuracy (Simpson et al. 2014). During KORUS-AQ, CO was measured by a fast-response (1 s) NASA Langley Differential Absorption Carbon monoxide Measurement (DACOM) instrument, with 1% measurement precision and 2% accuracy (Warner et al. 2010; Simpson et al. 2020).

Background air sampling

For all pre- and post-phaseout campaigns, background CFC-11 levels were based on measurements made at comparable latitudes and times in the remote Pacific basin, as part of the UCI long-term global trace gas monitoring program (Simpson et al. 2012). Background sampling locations include the islands of Kauai and Hawaii, USA (20–22°N); the west coast of Baja California, Mexico (22–31°N) and the west coasts of California, Oregon and Washington, USA (36–47°N). Table 1 shows the number of background samples per campaign and their locations.

An internal CFC-11 calibration review was completed by the UCI laboratory in 2021, which revealed a calibration

error in UCI's global long-term monitoring program for CFC-11 beginning in 2014, due to a data entry error. All affected measurements have been corrected by a factor of 1.0114. The correction is limited to the UCI long-term monitoring program (background measurements) and does not apply to other CFC-11 measurements made by UCI, including the urban studies presented here.

Results

CFC-11 levels in each city are presented below and compared to background measurements made at a similar time and latitude, and to an arbitrary value of 'background + 20%' as a simple way of comparing relative CFC-11 enhancements among the different datasets. CFC-11 enhancements are also compared with those of other trace gases to investigate potential source influences.

Pre-phaseout CFC-11 enhancements

While post-phaseout measurements are necessary to understand the unexpected recent increase in CFC-11 emissions, pre-phaseout CFC-11 data are rare in many urban areas and provide context for the range of CFC-11 concentrations that occurred before regulations took effect.

China: 45-city study and Beijing

1. *Forty-five city study (January–February, 2001)*. During the 45-city study in China, CFC-11 levels in most cities were within background + 20% (Fig. 3), averaging 289 ± 56 pptv or approximately $1.10 \times$ background overall (Table 2). Average CFC-11 levels were greater than background + 20% in two cities (Hangzhou, Jinan), and maximum levels were greater than background + 20% in six cities (Fig. 3). The maximum CFC-11 mixing ratio was 715 pptv ($2.8 \times$ background) in Hangzhou (Table 2), and the average in Hangzhou was 489 ± 134 pptv, based on five samples (Fig. 3). The cities with elevated CFC-11 levels were scattered throughout China (Fig. 3, inset), indicating that CFC-11 usage was common at that time. Because the 45-city study is based on 2–6 samples per city, the results are not intended to be comprehensive city-wide averages. Instead, they represent a snapshot of pre-phaseout CFC-11 levels based on a random wintertime sampling in China.
2. *Beijing Olympics (2008)*. The Beijing Olympics study occurred within the staggered phaseout period for CFCs prior to 2010, which included an 85% reduction by January 1, 2007 for Article 5 countries (see Introduction). During the study, average CFC-11 mixing ratios were higher in samples collected at Beijing CRAES (338 ± 125 pptv; $n = 37$) and Beijing city center (329 ± 39 pptv; $n = 150$) than in rural Xicicun (281 ± 46 pptv; $n = 37$) or mountainous Heishanzhai (279 ± 27 pptv; $n = 108$)

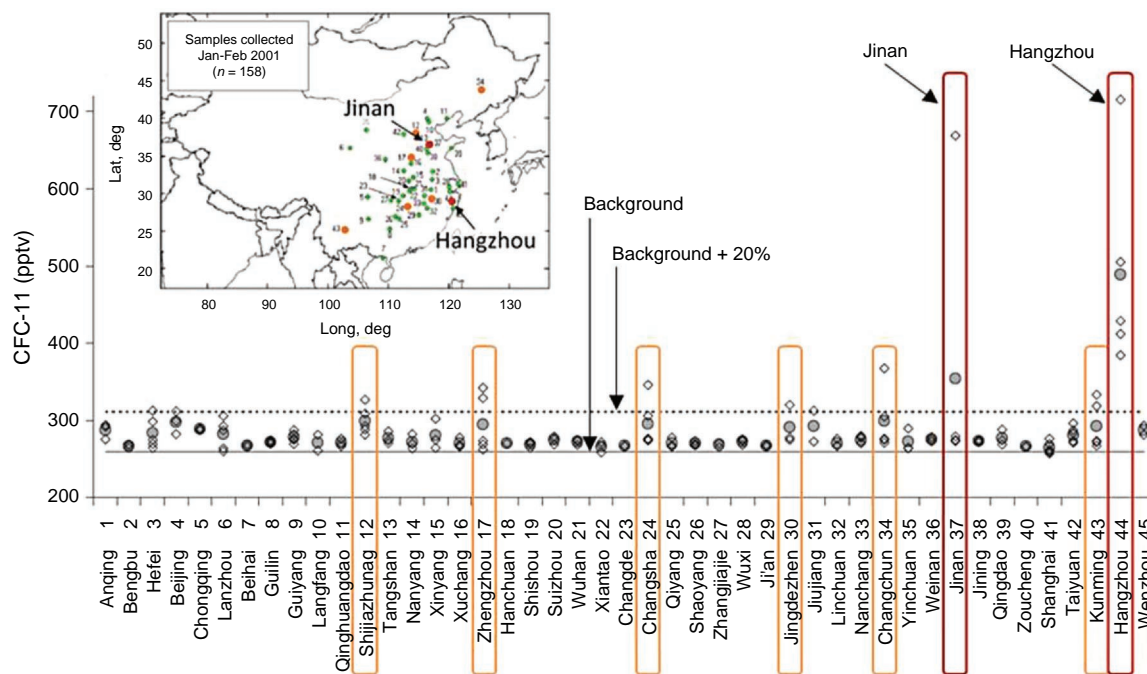


Fig. 3. Pre-phaseout CFC-11 mixing ratios during the 45-city study in China (January–February, 2001; $n = 158$). Open diamonds = individual samples, filled circles = city averages, solid line = background, dashed line = background +20%. Orange (red) rectangles highlight cities with individual (average) mixing ratios greater than background +20%; the same colours are used in the inset map.

(Fig. 4). The background CFC-11 level for this study was 242 ± 2 pptv and background +20% was 290 pptv. The average CFC-11 levels at Beijing CRAES, Beijing city center, Xicicun and Heishanzhai were $1.40\times$, $1.36\times$, $1.16\times$ and $1.16\times$ background, respectively, with a maximum of 1456 pptv at CRAES or $6.0\times$ background (Table 2). The overall CFC-11 average during the Beijing Olympics study was 313 ± 93 pptv or $1.3\times$ background, and the median (292 pptv) was $1.21\times$ background. These results show that CFC-11 levels were consistently elevated in Beijing during the timeframe of the 2008 Olympics, and that while elevated mixing ratios occurred in a widespread region around Beijing, they were especially elevated in the Beijing core including the Beijing city center and CRAES site.

Pakistan: Karachi

During the 1998/1999 and 2006 campaigns, most CFC-11 mixing ratios in Karachi were within 20% of background (Fig. 5). The average CFC-11 level in Karachi was 306 ± 48 in 1998/1999 ($1.16\times$ background) and 277 ± 31 pptv in 2006 ($1.11\times$ background) (Table 2). The 1998/1999 study occurred before the phaseout of CFCs in Article 5 countries, and the 2006 study occurred after the timeline of 50% CFC reduction by January 1, 2005 (see Introduction above). During both campaigns, average CFC-11 levels in Karachi were 4–11% higher in industrial areas than at roadside or urban locations, although the results were not statistically

significant. Maximum CFC-11 levels were 605 and 486 pptv in 1998 and 2006, respectively, or 2.3 and $2.0\times$ background (Table 2).

Pre-phaseout CFC-11 levels were higher in China than in Karachi, especially during the Beijing Olympics study (Fig. 5c). This occurred even though the 2008 Beijing Olympics study occurred within the timeframe of 85% reduction of CFCs, compared to 50% for the 2006 Karachi study. By contrast, overall VOC levels were much lower in China than Karachi. For example, median levels of ethane, one of the top three most abundant VOCs in each study, were $10\times$ higher in Karachi in 1998 than China in 2001, and $12\times$ higher in Karachi in 2006 than Beijing in 2008 (Fig. 5c). That is, CFC-11 levels were higher in Beijing than Karachi, even though overall VOCs levels were higher in Karachi during these pre-phaseout studies.

Post-phaseout CFC-11 enhancements

The post-phaseout studies took place from 2012 to 2018, when global CFC-11 concentrations had begun to decline more slowly than expected (Montzka *et al.* 2018).

Pakistan: Lahore

Lahore (2012). Unlike pre-phaseout CFC-11 measurements in Karachi, all post-phaseout mixing ratios in the 2012 Lahore study were below background +20% (Fig. 6). The average Lahore mixing ratio (253 ± 11 pptv)

Table 2. Statistics of CFC-II mixing ratios during urban field campaigns from 1998 to 2018.

Country	City	Average Date (year)	Bkgd CFC-II (pptv)	Min CFC-II (pptv)	Max CFC-II (pptv)	Median CFC-II (pptv)	Average CFC-II (pptv)	Average/Bkgd (pptv/pptv)	Max/Bkgd (pptv/pptv)	Count
Pre-phaseout (before 2010)										
Pakistan	Karachi	1999.0	262.8 (2.9)	264	605	292	306 (48)	1.16	2.30	80
Pakistan	Karachi	2006.0	248.6 (2.1)	253	486	267	277 (31)	1.11	1.96	83
China	45 city	2001.1	261.7 (1.7)	257	715	274	289 (56)	1.10	2.73	158
China	Beijing	2008.6	241.6 (2.3)	241	1456	292	313 (93)	1.30	6.03	332
Post-phaseout (after 2010)										
Saudi Arabia	Mecca	2012.8	235.4 (4.8)	244	268	257	256 (6)	1.09	1.14	46
Saudi Arabia	Medina	2012.8	235.4 (4.8)	240	282	261	261 (11)	1.11	1.20	21
Saudi Arabia	Jeddah	2012.8	235.4 (4.8)	251	269	259	260 (7)	1.10	1.14	10
Pakistan	Lahore	2012.9	235.0 (4.9)	236	278	252	253 (11)	1.08	1.18	48
Saudi Arabia	Mecca	2013.3	234.6 (2.9)	230	249	238	239 (6)	1.02	1.06	26
Saudi Arabia	Medina	2013.3	234.6 (2.9)	232	252	240	241 (6)	1.03	1.07	11
Saudi Arabia	Jeddah	2013.3	234.6 (2.9)	232	375	238	249 (34)	1.06	1.60	17
Saudi Arabia	Mecca Landfill	2013.4	234.6 (2.9)	246	658	437	417 (174)	1.78	2.80	5
Saudi Arabia	Mecca	2013.8	234.6 (5.1)	235	260	248	247 (7)	1.05	1.11	20
Saudi Arabia	Jeddah	2013.8	234.6 (5.1)	241	268	255	255 (7)	1.09	1.14	16
Nepal	Bode	2015.3	233.0 (2.5)	230	286	239	247 (17)	1.06	1.23	9
Nepal	Garbage burning	2015.4	233.0 (2.5)	230	626	273	341 (149)	1.46	2.69	6
Nepal	Kathmandu	2018.3	228.3 (3.2)	225	300	240	243 (14)	1.06	1.31	35
China	Mount Tai	2014.5	235.8 (5.8)	234	360	263	267 (22)	1.13	1.53	70
China	Tuoji Island	2014.9	233.8 (5.9)	230	290	240	245 (15)	1.05	1.24	48
China	Dongying	2016.7	231.6 (2.1)	236	388	277	286 (37)	1.23	1.68	49
China	Qingdao	2018.2	229.4 (4.3)	231	279	247	251 (15)	1.09	1.22	32
China (KORUS)	Yellow Sea	2016.4	231.6 (3.0)	234	295	251	254 (14)	1.10	1.27	66
South Korea	Seoul	2015.4	232.6 (3.1)	237	341	255	264 (24)	1.13	1.47	23
South Korea	Seoul	2016.4	231.6 (3.0)	227	362	253	258 (23)	1.11	1.56	177
South Korea	Daesan	2016.4	231.6 (3.0)	237	260	251	251 (6)	1.08	1.12	41
South Korea	Busan	2016.4	231.6 (3.0)	228	246	233	235 (4)	1.01	1.06	32

Numbers in parentheses are 1σ . 'Phaseout' refers to 100% reduction of CFC production/consumption by January 1, 2010. Note that the Karachi (2006) and Beijing (2008) studies straddled the gradual CFC reduction period prior to 2010 (see text).

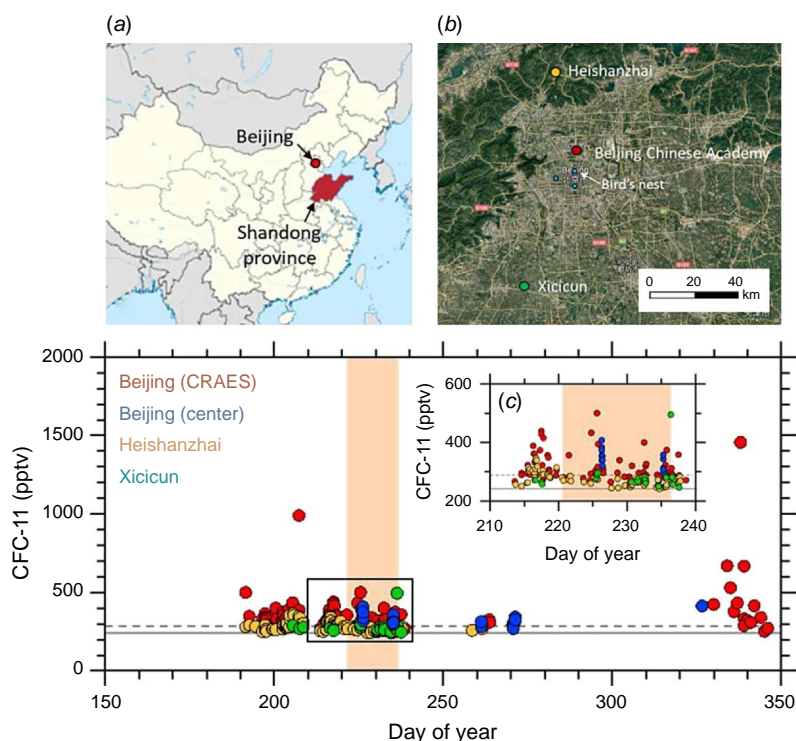


Fig. 4. Pre-phaseout CFC-11 mixing ratios in China during the Beijing Olympics study (July–November, 2008). (a) Map of China; (b) sampling sites in the Beijing area; (c) CFC-11 mixing ratios during the Beijing Olympics Study. (b, c): Red = CRAES; blue = Beijing city center; orange = Heishanzhai; green = Xicicun, (c): Solid line = background, dashed line = background +20%, orange shading = Beijing Olympics from August 8–24, 2008. Shandong Province (studied in 2014–2018) is also shown in (a). The inset in (c) shows detail during the timeframe of the Beijing Olympics.

was $1.08 \times$ the background of 235 ± 5 pptv, and the maximum (278 pptv) was $1.18 \times$ background (Table 2). There was no statistically significant difference between CFC-11 measurements in urban, suburban, roadside or industrial spaces of Lahore. Although the pre-phaseout and post-phaseout measurements in Pakistan were taken in different cities, the average CFC-11 abundance declined from $1.16 \times$ background in 1998/1999, to $1.11 \times$ background in 2006, and to $1.08 \times$ background in 2012 (Table 2). The maximum CFC-11 values also decreased from $2.30 \times$ to $1.96 \times$ to $1.18 \times$ background over the same period. While the measurements are sparse, this snapshot is consistent with reduced CFC-11 emissions over time (Ul-Haq *et al.* 2016).

As with the Karachi studies, the relatively low CFC-11 enhancements in Lahore occurred despite an abundance of other VOCs. For example, ethane was the most abundant VOC measured in Lahore, with a median mixing ratio of 34.9 ppbv or $22 \times$ background (Barletta *et al.* 2017). CFC-11 correlated poorly with other compounds measured in Lahore. Its best correlation was with CFC-12 ($r^2 = 0.37$) and it had little correlation with other species such as CCl_4 ($r^2 = 0.07$) or CO ($r^2 = 0.12$) (Fig. 6c–e). Overall, these results suggest low levels of CFC-11 emissions throughout Lahore in 2012, despite abundant levels of CO (up to 17.9 ppmv) and numerous VOCs.

Saudi Arabia: Mecca, Medina and Jeddah

Multiple air sampling campaigns were carried out in western Saudi Arabia from 2012 to 2013 (as detailed in *Saudi Arabia (2012, 2013): Mecca, Medina, Jeddah*

($n = 172$) above). Sampling locations are shown in Fig. 7a, b, and results in Fig. 7c–f.

1. *Mecca/Medina/Jeddah: Hajj (October–November 2012)*. During the first Hajj campaign, all urban CFC-11 mixing ratios in Mecca, Medina and Jeddah stayed within 20% of background (Fig. 7c). Average CFC-11 levels were 1.09 – $1.11 \times$ background, and maximum values were 1.14 – $1.20 \times$ background (Table 2). (Note that a higher CFC-11 maximum of 433 pptv was published in Simpson *et al.* (2014) based on a tunnel sample that is not included here.)

By comparison to CFC-11, many other VOCs were strongly elevated during the 2012 Hajj campaign. For example, i-pentane was the most abundant VOC measured in Mecca, with an average of 42 ± 17 ppbv in urban (non-tunnel) spaces of Mecca, or $325 \times$ background (Simpson *et al.* 2014). Therefore, as with the Lahore study in 2012, the CFC-11 levels in western Saudi Arabia remained fairly low despite remarkably abundant levels of other VOCs.

2. *Mecca/Jeddah: Hajj (October 2013)*. CFC-11 levels in Mecca and Jeddah during the 2013 Hajj campaign were again within 20% of background (Fig. 7d), with average values of 1.05 – $1.09 \times$ background and maximum values of 1.11 – $1.14 \times$ background (Table 2). The 2013 Mecca sampling focused more on tunnel sampling, so fewer urban samples were collected than in 2012. As in 2012, abundant levels of other VOCs were not associated with elevated CFC levels.

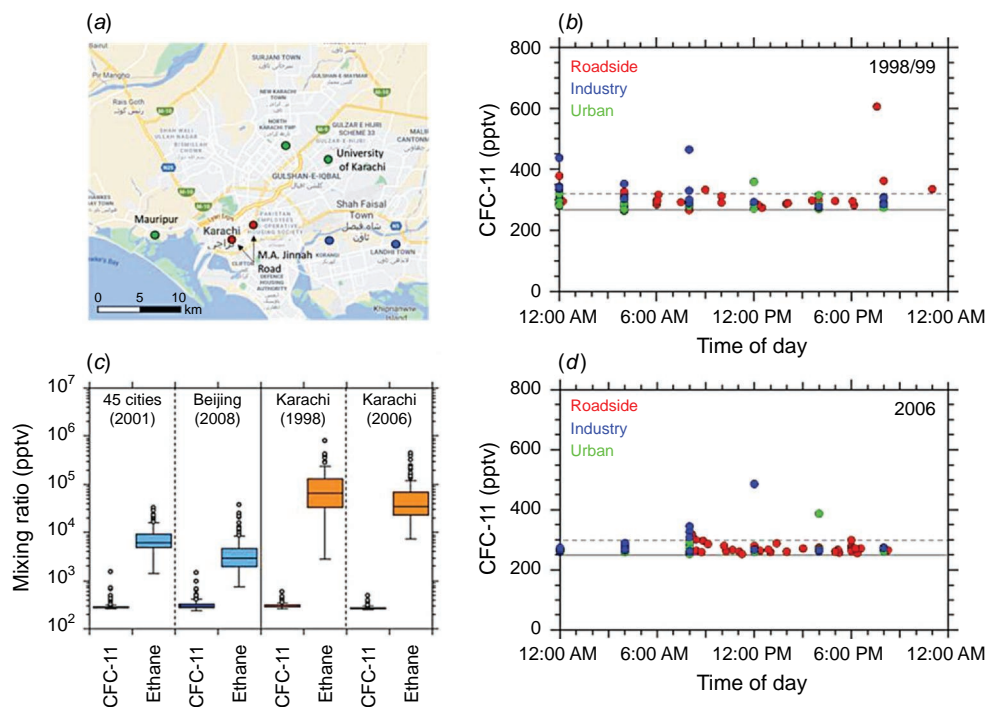


Fig. 5. Pre-phaseout CFC-11 mixing ratios in Karachi, Pakistan. (a) Sampling sites in Karachi; (b) CFC-11 mixing ratios in Karachi from December 1998 to January 1999; (c) comparison of pre-phaseout levels of CFC-11 and ethane in China (45 cities in 2001; Beijing in 2008) and Karachi; (d) CFC-11 mixing ratios in Karachi in January 2006. (a, b, d): Red = roadside, blue = industry, green = urban. (b, d): Solid line = background, dashed line = background +20%. (c): Blue = China, orange = Karachi. Each box in (c) encloses 50% of the data (the interquartile distance, IQD); median = horizontal line; whiskers = minimum and maximum, except for outliers (open circles) which are values greater than the third quartile plus 1.5 times the IQD.

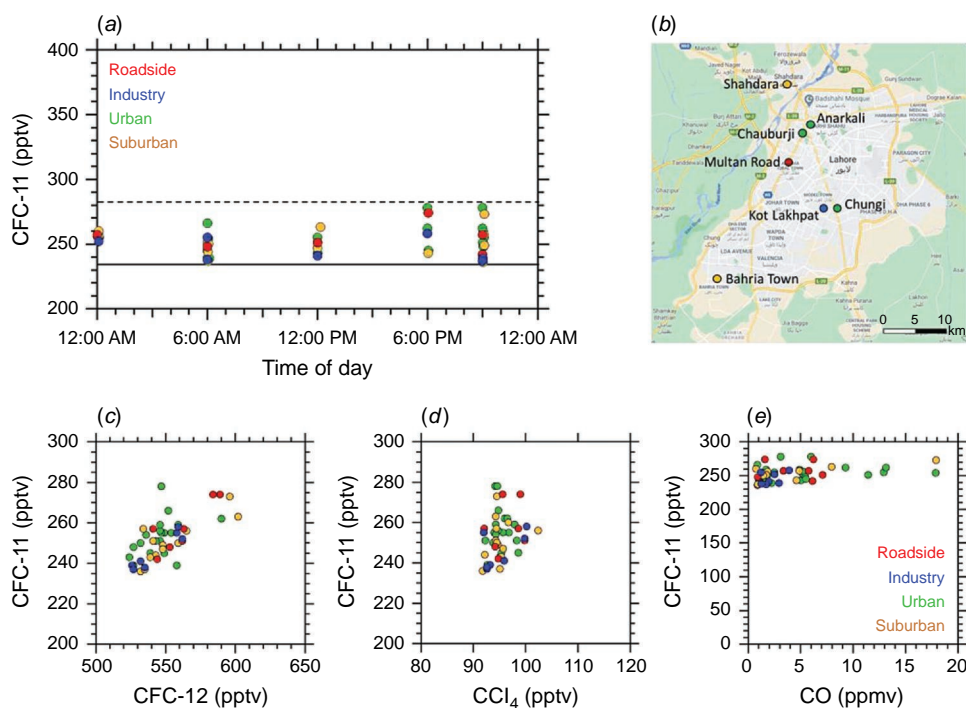


Fig. 6. Post-phaseout CFC-11 mixing ratios in Lahore, Pakistan in December 2012. (a) CFC-11 mixing ratios vs. time of day; solid line = background, dashed line = background +20%; (b) sampling sites in Lahore; (c–e) CFC-11 correlations with CFC-12, CCl₄ and CO. Red = roadside; blue = industry; green = urban; orange = suburban.

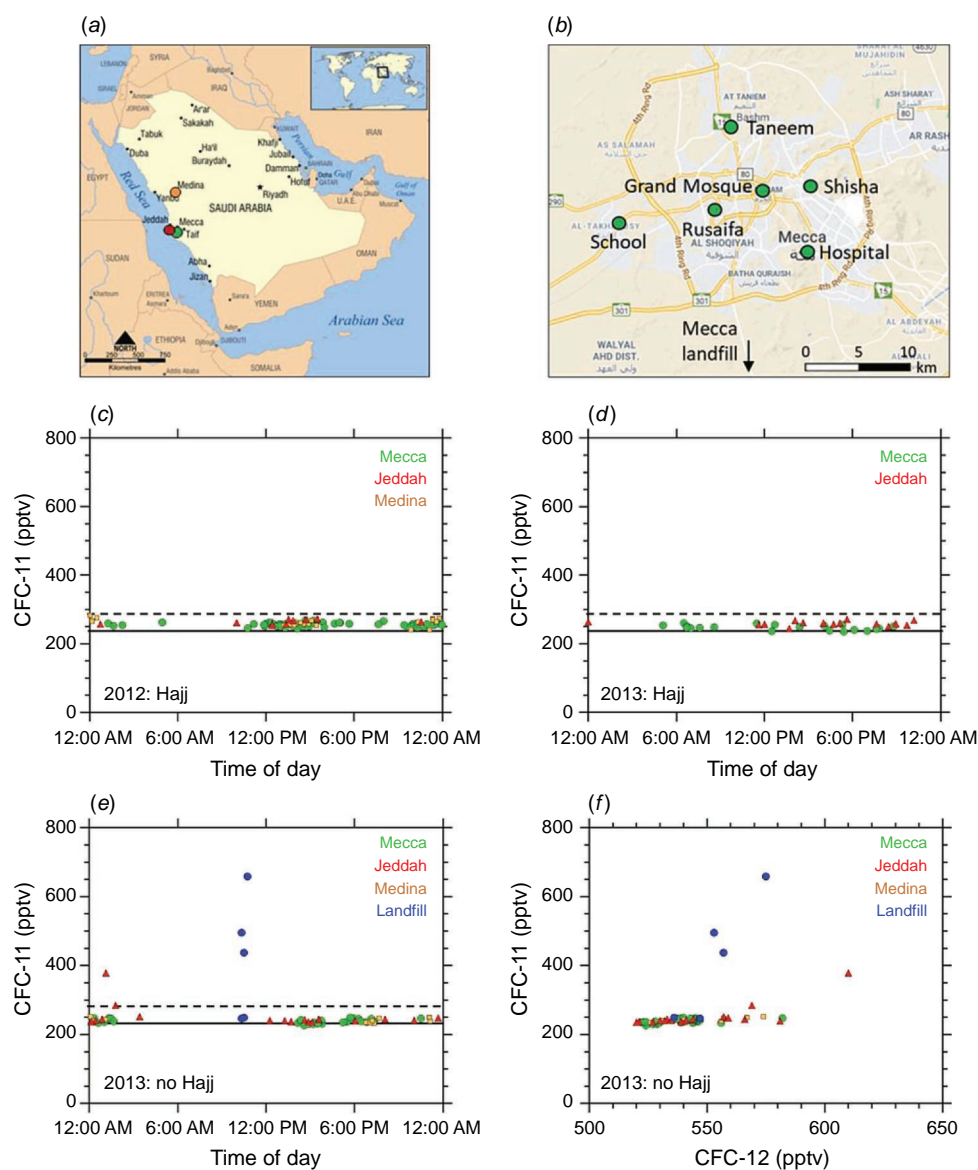


Fig. 7. CFC-11 mixing ratios in western Saudi Arabia during campaigns from 2012 to 2013. (a) Map of Saudi Arabia, including Mecca, Jeddah and Medina; (b) sampling locations in Mecca; (c–e) CFC-11 vs time of day during (c) the October–November 2012 Hajj campaign, (d) the October 2013 Hajj campaign, and (e) the April 2013 campaign (non-Hajj), including the landfill fire in May 2013; (f) correlations between CFC-11 and CFC-12 in April–May 2013. Green = Mecca; red = Jeddah; orange = Medina; blue = landfill. Panels (c–e): solid line = background; dashed line = background +20%.

3. *Mecca/Medina/Jeddah: non-Hajj (April 2013).* A non-Hajj study was conducted in April, 2013, midway between the two Hajj campaigns (Fig. 7e). With the exception of a CFC-11 maximum in Jeddah (discussed below) the results were similar to the Hajj campaigns. The CFC-11 averages in Mecca, Medina and Jeddah were $1.02\text{--}1.06\times$ background, and the maximum values in Mecca and Medina were $1.06\text{--}1.07\times$ background (Table 2). All Jeddah values were within background +20%, except the Jeddah maximum (375 pptv or $1.60\times$ background)

measured in the Al Mahjar district, which includes commercial and industrial activities. A lower CFC-11 value (258 pptv) was measured in this district during the 2013 Hajj campaign, and further work is needed to characterise the frequency of elevated CFC-11 levels in this area of Jeddah, and whether they still persist. It is also important to note that low-level CFC-11 emissions are expected post-phaseout from existing banks of CFC-11, and that elevated values do not necessarily indicate non-compliance. Overall, almost all of the non-Hajj results

were within background +20%, despite abundant levels of other VOCs even without the additional activities of Hajj (Simpson et al. 2014).

4. *Landfill fire, Mecca (May 2013)*. The Mecca landfill is located about 20 km south of the Grand Mosque (Fig. 7b). It receives several thousand tons of solid waste on normal days, primarily organic waste and plastics (Anjum et al. 2016). Because it is used to dump waste and does not have leachate or gas collection infrastructure, it is technically a non-engineered landfill (Anjum et al. 2016).

Five air samples were collected from an unexpected fire at the Mecca landfill on May 13, 2013 (Fig. 7e, f). CFC-11 was notably elevated in 3 of 5 of the landfill fire samples, with values reaching 437–658 pptv or 1.9–2.8 × background (Samples 1, 4 and 5 in Table 3). CO was relatively low in Sample 1 (2 × background) while Samples 4 and 5 were heavily impacted by smoke (CO = 155–205 × background). Landfills are known to be a repository of CFC-11 products such as blown foams (Hodson et al. 2010), and garbage burning and landfill fires can be a source of CFC-11 when they re-suspend CFC-11 contained within the garbage products. Fires can also re-suspend previously deposited pollutants such as CFCs (Hegg et al. 1990). Because CFC-11 is only present in certain components of landfill fuel, whereas CO and VOCs are emitted more ubiquitously, it appears reasonable that CFC-11 was preferentially detected in certain samples. Indeed, CO correlated well with a large number of compounds ($r^2 > 0.90$ for 50 VOCs) whereas CFC-11 correlated well with relatively few species including CFC-12 ($r^2 = 0.85$; Fig. 7f).

Fraser et al. (2020) discuss CFC emissions from landfills based on studies in Australia, Europe and the USA. They note that emissions of CFC-11 from modern landfills are relatively low because of good containment technology and because of substantial CFC-11 biodegradation in landfills due to the high number of chlorine atoms per CFC-11 molecule (Scheutz et al. 2007). As a result, landfill gas often contains an excess of CFC-12 compared to CFC-11. Here, however, the Mecca landfill

is not engineered and may not lend itself to effective CFC-11 decomposition. The relative excess of CFC-11 compared to CFC-12 in Samples 1, 4 and 5 (201–422 pptv for CFC-11 vs 30–52 pptv for CFC-12; Table 3) suggests that the landfill components were richer in CFC-11 than CFC-12 and/or had less time for the CFC-11 to anaerobically degrade before being re-suspended during the fire. Open burning in dumps is a common practice and landfill fires occur frequently, with more than 8000 landfill fires per year even in the USA (US Fire Administration 2001; Gullett et al. 2010). Further investigation of fires at dumps and landfills is encouraged to determine their global impact on CFC emissions.

Nepal: Kathmandu and Bode

Sampling locations for the 2015 and 2018 campaigns in Nepal are shown in Fig. 8a. The 2015 campaign had fewer samples than planned because of the Gorkha Earthquake (see details given in the Nepal (2015, 2018): Kathmandu/Bode ($n = 50$) section above).

1. *Kathmandu/Bode (April and June, 2015)*. The average CFC-11 mixing ratio in the suburban Bode samples was 247 ± 17 pptv, or $1.06 \times$ background, and the maximum was 286 pptv or $1.23 \times$ background (Table 2). The maximum sample had elevated levels of other halocarbons such as tetrachloroethene or C_2Cl_4 (75 pptv vs a median of 6 pptv) and HCFC-141b or CH_3CCl_2F (123 pptv vs a median of 29 pptv), suggesting some urban/industrial influence. Average CFC-11 levels were relatively low in background samples that were collected locally in Nepal (237 ± 6 pptv, or $1.02 \times$ the Pacific background), but elevated CO levels in some of these samples indicate that they were not pristine (Fig. 8b). Unlike the measurements in Lahore and western Saudi Arabia, the Bode samples did not contain remarkably elevated levels of other VOCs, which is reasonable for this suburban location. For example, the *i*-pentane maximum in Bode was 6 ppbv, compared to 222 ppbv in Lahore and 851 ppbv in Mecca in April 2013 (Fig. 9). Bearing in mind the

Table 3. Statistics of CO and selected VOCs in samples collected from a fire at the Mecca landfill on May 26, 2013.

#	Time	CO (ppbv)	CFC-11 (pptv)	CFC-12 (pptv)	CCl_4 (pptv)	Ethene (pptv)	Ethyne (pptv)	Benzene (pptv)
Bkgd	n/a	88 ± 8	236 ± 2	523 ± 3	85 ± 1	84 ± 46	56 ± 10	19 ± 14
1	10:20	160	495	553	87.7	440	440	372
2	10:20	289	246	547	84.9	2392	1183	488
3	10:30	1475	249	536	84.5	67 561	5318	61 149
4	10:30	18 198	437	557	88.4	1 317 690	61 004	1 180 410
5	10:44	13 586	658	575	85.3	673 639	41 283	466 662

= sample number. Bkgd = average ($\pm 1\sigma$) background from Mexico and Hawaii (20–25°N) in March and June, 2013 ($n = 12$). Note that numbers have not been rounded and may be beyond their measurement precision (1% for halocarbons, 2% for CO, and 3% for hydrocarbons).

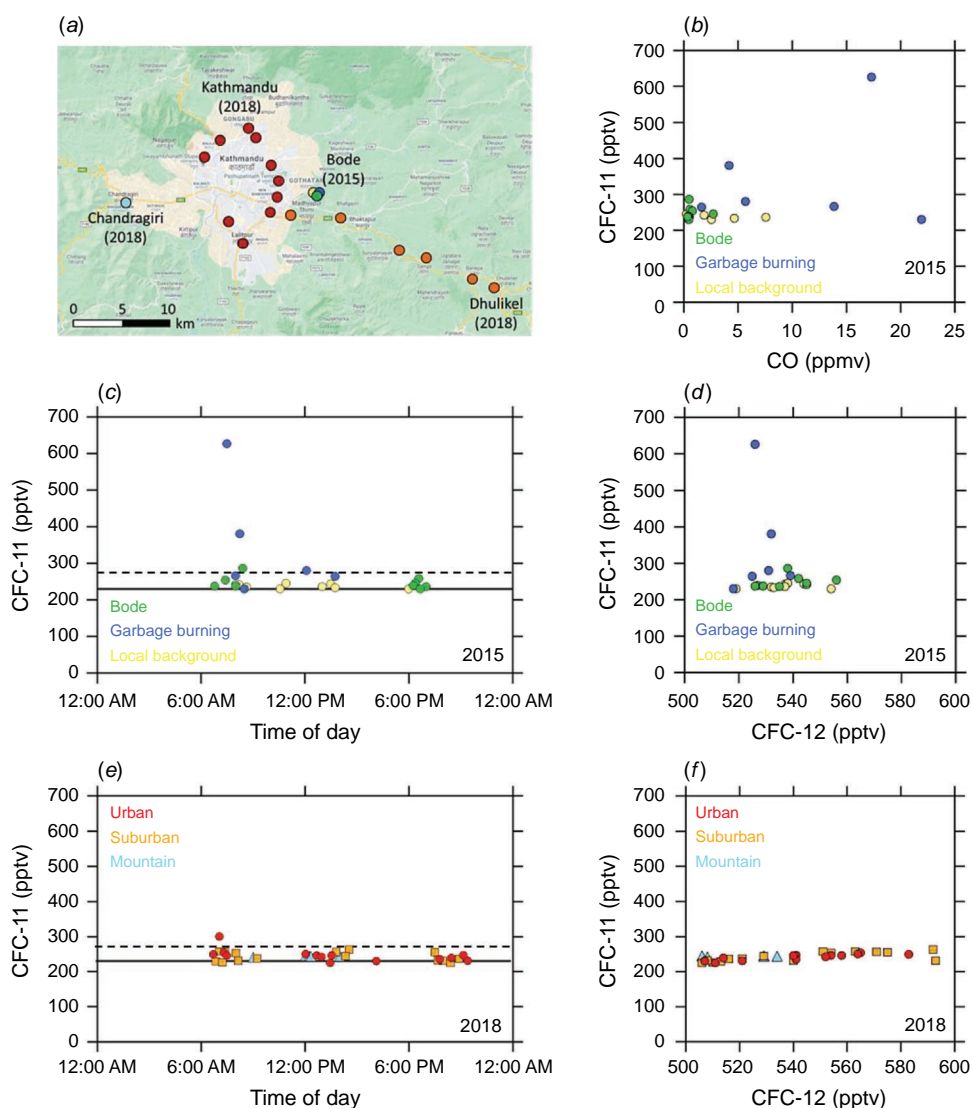


Fig. 8. CFC-11 mixing ratios in Nepal in April–June, 2015 and April 2018. (a) Sampling sites in Kathmandu and surrounding area. *Campaign in 2015*: (b) CFC-11 vs CO; (c) CFC-11 vs time of day; (d) CFC-11 vs CFC-12. Green = Bode; blue = garbage burning; yellow = local background. *Campaign in 2018*: (e) CFC-11 vs time of day; (f) CFC-11 vs CFC-12. Red = urban; orange = suburban; light blue = mountain. Panels (c, e): solid line = background; dashed line = background +20%.

relatively small sample size, this analysis indicates generally low CFC-11 levels in suburban Bode.

2. *Garbage burning (April and June, 2015)*. Garbage burning is a common and poorly regulated practice in South Asia (Kumar *et al.* 2020). The 2015 Nepal study included limited sampling of different types of garbage burning (see *Nepal (2015, 2018): Kathmandu/Bode* section above). The average CFC-11 mixing ratio in the garbage burning samples was 341 ± 149 pptv or $1.5 \times$ background, with a maximum of 626 pptv or $2.7 \times$ background (Fig. 8b–d, Table 2). That is, average and maximum CFC-11 levels were much higher in the garbage burning samples than in the suburban Bode samples.

The CFC-11 maximum in the Nepal garbage fires (626 pptv) was similar to Mecca landfill fire maximum (658 pptv), but unlike the Mecca landfill fire, CFC-12 was not elevated in the Nepal garbage burning samples and did not correlate with CFC-11 ($r^2 < 0.01$; Fig. 8d). This is likely because the Nepal garbage fires were relatively small and would not have the wider variety of garbage products as the Mecca municipal landfill, including those containing CFC-12 as refrigerants.

While five of six garbage burning samples produced CFC-11 levels above background, including three above background +20%, not all garbage fires sampled in Nepal emitted CFC-11 (Table 4). The CFC-11 mixing

ratio was 230 pptv, or at background levels, in a sample from a garbage fire characterised as ‘huge’, with contents including plastic, newspaper and shoes, and with CO levels of almost 22 000 ppbv (Table 4). The highest CFC-11 mixing ratio (626 pptv) was recorded from a roadside garbage fire with mixed contents (cardboard, cans, cloth, cigarette packets, etc.), and the second-highest (380 pptv) from a flaming fire that included plastic bags and cardboard. As in the case of the Mecca landfill fire, the elevated CFC-11 in these fires suggests the likelihood of additional garbage components such as blown foam, which retains CFC-11 within the foam cells (Harris et al. 2019; Lickley et al. 2020). Detailed fuel content is given in Stockwell et al. (2016), but the sample size was too small to determine consistent trends with respect to fuel content. Overall, these results show that CFC-11 is emitted from garbage burning sources in Nepal in a post-phaseout timeframe and that CFC-11 emissions vary from fire to fire.

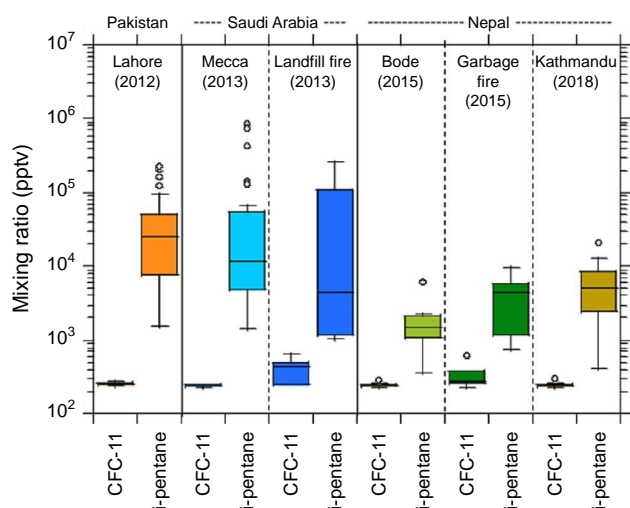


Fig. 9. Comparison of post-phaseout levels of CFC-11 and *i*-pentane in Lahore, Pakistan (2015), western Saudi Arabia (April 2013) and the Kathmandu region of Nepal (2015, 2018), including the Mecca landfill fire and Bode garbage burning samples. The box-whisker plot is described in Fig. 5.

Crude emission estimates of CFC-11 from global garbage burning were calculated based on excess CFC-11/CO in the Nepal fires (8.2 ± 4.8 pptv/ppmv; $r^2 = 0.37$) and total CO emitted from global open waste burning ($37\,000$ Gg year⁻¹; Wiedinmyer et al. 2014), using Eqn 1:

$$E_{\text{CFC11}} = E_{\text{CO}} \times \frac{\text{MW}_{\text{CFC11}}}{\text{MW}_{\text{CO}}} \times \frac{\Delta\text{CFC11}}{\Delta\text{CO}} \quad (1)$$

where E is emissions of CFC-11 or CO in Gg year⁻¹, MW is molecular weight and $\Delta\text{CFC11}/\Delta\text{CO}$ is the excess of CFC-11 and CO over background. The $\Delta\text{CFC11}/\Delta\text{CO}$ value of 8.2 ± 4.8 pptv/ppmv was determined by subtracting off the background (116 ppbv for CO, 230 pptv for CFC-11) from each of the six samples shown in Table 4, then forcing a linear fit of these excess CO and CFC-11 values through zero (see Simpson et al. 2011 for details). The resulting global emission estimate calculation has numerous uncertainties, including small sample size, relatively low correlation between CFC-11 and CO, representativeness of Nepal for global emission estimates and so forth. Bearing this in mind, this rough calculation suggests a potential contribution of garbage burning to global CFC-11 emissions on the order of 1–2 Gg year⁻¹. A similar calculation can be done for the Mecca landfill fires (see results section *Saudi Arabia: Mecca, Medina and Jeddah* above). Here, however, we note that all five landfill samples were collected within a 30 min timeframe (Table 3), and so they represent less spatiotemporal variability than the Nepal garbage fires. Bearing this in mind, $\Delta\text{CFC11}/\Delta\text{CO}$ for the Mecca landfill fire was 18.3 ± 7.5 pptv/ppmv, to give a potential contribution of landfill fires to global CFC-11 emissions of 3–4 Gg year⁻¹. Together the Nepal garbage burning and Mecca landfill fire data suggest that open garbage burning and landfill fires could potentially emit CFC-11 in a rough range of 1–4 Gg year⁻¹ globally. However further work is needed for robust global emission estimates.

As indicated earlier, the presence of CFC-11 emissions is expected in a post-phaseout timeframe due to emissions from existing banks such as older foams. However, Chen et al. (2020) found less negative CFC-11 trends for

Table 4. Statistics of CO and selected VOCs in six samples collected from open garbage burning in Nepal in April and June, 2015.

#	Date	Time	CO (ppbv)	CFC-11 (pptv)	CFC-12 (pptv)	Ethene (pptv)	Ethyne (pptv)	Benzene (pptv)
Bkgd	Mar, Jun	n/a	116 ± 12	230 ± 3	520 ± 5	n/a	170 ± 105	47 ± 30
1	Apr 14	12:06	5703	280	531	186 140	60 410	35 390
2	Apr 24	13:45	1659	264	525	48 309	111 445	9248
3	Jun 6	07:30	17 315	626	526	416 367	61 633	199 872
4	Jun 6	08:00	13 862	266	539	334 540	67 891	116 145
5	Jun 6	08:15	4204	380	532	110 842	75 898	24 302
6	Jun 6	08:30	21,925	230	518	329 004	722 381	341 877

= sample number. Bkgd = average ($\pm 1\sigma$) background measurements from Mexico in March and June, 2015 ($n = 10$). Note that numbers have not been rounded as discussed in Table 3.

2013–2018 relative to 2003–2018 in five grid boxes, including Shandong province (slowdown of ~ 1 ppt year $^{-1}$), three grid boxes in the Arabian Peninsula (~ 1 ppt year $^{-1}$) and northern India, Pakistan and Nepal (~ 0.5 ppt year $^{-1}$). This suggested possible slowdowns of the CFC-11 trend in these regions since 2013 (Chen *et al.* 2020). The Mecca landfill fire and Bode garbage burning samples show the existence of CFC-11 sources in the Arabian Peninsula and Nepal regions during 2013–2018. Further information would be needed to determine whether such sources are substantial enough, and different enough in 2013–2018 relative to earlier periods, to have influenced the slower CFC-11 trends detected by AIRS. As stated in Chen *et al.* (2020), the coincidence of CFC-11 sources within the same region as statistically significant AIRS retrieval trends is worthy of further investigation.

3. *Kathmandu (April, 2018)*. The Kathmandu Valley was re-sampled in 2018, covering a broader region (for details see Nepal (2015, 2018): *Kathmandu/Bode* ($n = 50$) above). The average CFC-11 mixing ratio was 243 ± 14 pptv or $1.06 \times$ background, and the maximum was 300 pptv or $1.31 \times$ background (Fig. 8e, Table 2). These values are similar to those observed in Bode in 2015, suggesting low levels of CFC-11 emissions throughout the Kathmandu Valley with occasional values greater than background +20%. CFC-11 correlated well with CFC-12, HCFC-22 and other CFCs ($r^2 = 0.68$ – 0.77 ; Fig. 8f) and poorly with other gases ($r^2 < 0.45$). The CFCs and HCFC-22 are used as refrigerants and/or solvents, and their correlation with CFC-11 suggests co-located emissions in Kathmandu.

In contrast to CFC-11, mixing ratios of other VOCs were generally higher in samples spread across the Kathmandu Valley (2018) than the single suburban Bode location (2015), due to both urban enhancement and the closer proximity of Kathmandu samples to roads (Fig. 9). For example, average VOC levels in the Kathmandu Valley were $3 \times$ higher than in Bode for both the traffic tracer ethene and the gasoline evaporation tracer *i*-pentane. However, VOC levels in Kathmandu (2018) were lower than in Lahore, Pakistan (2012) or western Saudi Arabia (2012–2013), for example by 8 – $18 \times$ for *i*-pentane (Fig. 9). By contrast, average CFC-11 levels were similar among the three countries, ranging from 1.06 to $1.08 \times$ background in Bode, Kathmandu and Lahore, and 1.02 – $1.11 \times$ background in western Saudi Arabia (Table 2). In summary, similar urban CFC-11 enhancements were observed among the three countries, despite different VOC abundances. Stronger CFC-11 enhancements from municipal pyrogenic sources are worthy of further investigation.

China: Shandong Province

The four ground-based sampling campaigns in Shandong Province occurred within the timeframe and region where excess CFC-11 emissions were expected to be occurring

(Montzka *et al.* 2018; Rigby *et al.* 2019). Sampling locations are shown in Fig. 10a and results are discussed below.

1. *Mount Tai (June–July, 2014)*. CFC-11 mixing ratios at Mount Tai averaged 267 ± 22 pptv, or $1.13 \times$ background, with a maximum of 360 pptv or $1.5 \times$ background (Table 2). Elevated CFC-11 mixing ratios were measured throughout the June 4 to July 4 campaign, and 21% of samples were above background +20%.
2. *Tuoji Island (December, 2014)*. Of the four ground-based surveys in Shandong province, CFC-11 levels were least elevated at Tuoji Island, as may be expected for this comparatively remote location (see description in section *China (2014–2018): Shandong province* ($n = 199$) above). Average CFC-11 mixing ratios were 245 ± 15 pptv or $1.05 \times$ background, with a maximum of 290 pptv or $1.24 \times$ background (Table 2). Only two samples were greater than background +20% (Fig. 10b), with 48-h HYSPLIT back trajectories originating from the southwest over Shandong province. By comparison, back trajectories for the two lowest CFC-11 measurements arrived from the northwest.
3. *Dongying (September, 2016)*. Similar to Mount Tai, CFC-11 was relatively elevated in Dongying, with an average of 286 ± 37 pptv or $1.23 \times$ background, and a maximum of 388 pptv or $1.7 \times$ background (Table 2). This is the only urban post-phaseout campaign presented here with a CFC-11 average greater than $1.2 \times$ background, with 47% of samples above background +20%. For comparison, the Dongying average and maximum are lower than in pre-phaseout Beijing (313 ± 93 or $1.30 \times$ background, and 1456 pptv, respectively; Table 2). The CFC-11 average reported here is similar to those measured in 2017 at a site 32 km northeast of Dongying, with values of 274 ± 26 pptv in summer and 302 ± 79 pptv within oil fields (Zheng *et al.* 2019).
4. *Qingdao (March–April, 2018)*. The Qingdao CFC-11 results were similar to Tuoji Island, with relatively lower CFC-11 enhancements compared to Mount Tai or Dongying. The average was 251 ± 15 pptv, or $1.09 \times$ background, with a maximum of 279 pptv or $1.22 \times$ background (Table 2). Qingdao was also measured during the 45-city survey of China in 2001 (see *China: 45-city study and Beijing* section above), with a CFC-11 average of 277 ± 10 pptv or $1.07 \times$ background ($n = 3$). Bearing in mind the very limited sample size and duration, the 2001 and 2018 results both suggest that Qingdao is not a major CFC-11 emission location within Shandong province.

Overall, average CFC-11 mixing ratios were $1.13 \times$ background at Mt Tai (2014), $1.05 \times$ background on Tuoji Island (2014), $1.23 \times$ background in Dongying (2016) and $1.09 \times$ background in Qingdao (2018). Other studies during this timeframe also measured elevated CFC-11 concentrations

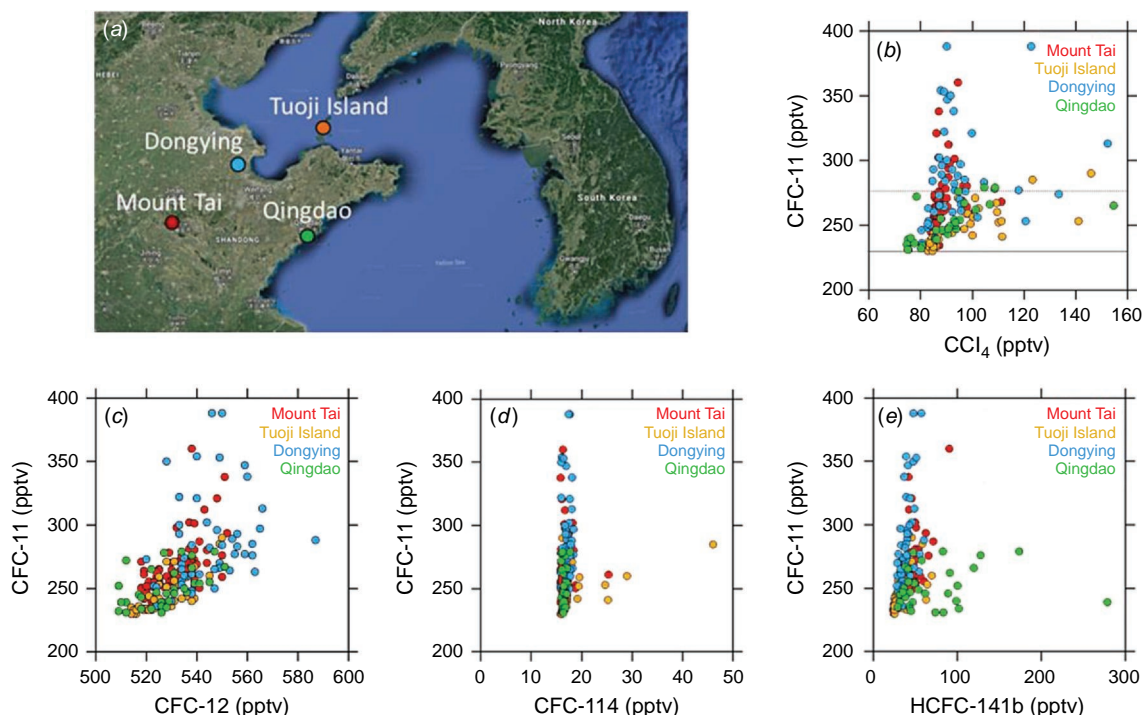


Fig. 10. CFC-11 mixing ratios measured in Shandong Province, China from 2014 to 2018. (a) Map of sampling sites; CFC-11 vs (b) CCl_4 ; (c) CFC-12; (d) CFC-114; (e) HCFC-141b. Red = Mount Tai (2014); orange = Tuoji Island (2014); blue = Dongying (2016); green = Qingdao (2018).

(Lin et al. 2019; Benish et al. 2021; Yi et al. 2021). Benish et al. (2021) reported an average CFC-11 mixing ratio of 351 ± 358 pptv, or $1.52 \times$ background, based on 27 airborne whole air samples collected over Hebei province in spring 2016. Yi et al. (2021) reported that CFC-11 reached its highest value in 2016 (279 ± 30 pptv, or $1.20 \times$ background) based on surveys in five cities in China (Beijing, Hangzhou, Guangzhou, Langzhou and Chengdu) from 2009 to 2019. Bearing in mind the different survey locations, the results reported here in 2016 ($1.23 \times$ background in Dongying) are similar to those reported by Yi et al. (2021) in 2016 and lower than those of Benish et al. (2021).

Fig. 10 shows correlations between CFC-11 and other halocarbons during the Shandong campaigns. CFC-11 and the other halocarbons showed some correlation on Tuoji Island ($r^2 = 0.25\text{--}0.61$) and relatively poor correlation elsewhere ($r^2 < 0.4$), suggesting CFC-11 was largely released independently of other chlorinated compounds. CCl_4 is a feedstock for CFC-11 production (see Introduction) and CFC-11 vs CCl_4 shows two distinct wings, with relatively abundant CFC-11 in Mount Tai and Dongying, and relatively abundant CCl_4 in Tuoji Island and Qingdao (Fig. 10b). Their overall lack of correlation suggests that the elevated CFC-11 did not result from CFC-11 emission during production from CCl_4 . Consistent with this, release of CFC-11 may occur during or after foam blowing, rather than earlier during its production stage (Rigby et al. 2019).

South Korea: Seoul, Daesan, Busan and outflow from China

The locations of air samples collected in South Korea are shown in Fig. 11a, and detailed flight tracks for KORUS-AQ are presented in Simpson et al. (2020).

1. *Seoul (May–June, 2015)*. CFC-11 levels in ground-based samples during the 2015 MAPS-Seoul campaign averaged 264 ± 24 pptv, or $1.13 \times$ background (Table 2, Fig. 11c). This enhancement is larger than average post-phaseout urban enhancements in the Kathmandu region of Nepal ($1.06 \times$ background), Lahore, Pakistan ($1.08 \times$) and western Saudi Arabia ($1.02\text{--}1.11 \times$), and within the range for Shandong Province ($1.05\text{--}1.23 \times$). The maximum CFC-11 level during MAPS-Seoul was 341 pptv, or $1.47 \times$ background, also within the range of Shandong Province values ($1.22\text{--}1.68$) and similar to Jeddah in spring, 2013 ($1.60 \times$).
2. *KORUS-AQ (May–June, 2016)*. Air over South Korea was sampled extensively during KORUS-AQ, including low-altitude sampling over Seoul, Daesan and Busan (see South Korea (2015, 2016): MAPS-Seoul, KORUS-AQ ($n = 2577$) section above for details).

2a. *Seoul (May–June, 2016)*. Average CFC-11 levels in low-altitude samples over Seoul were 258 ± 23 pptv or $1.11 \times$ background, and the maximum was

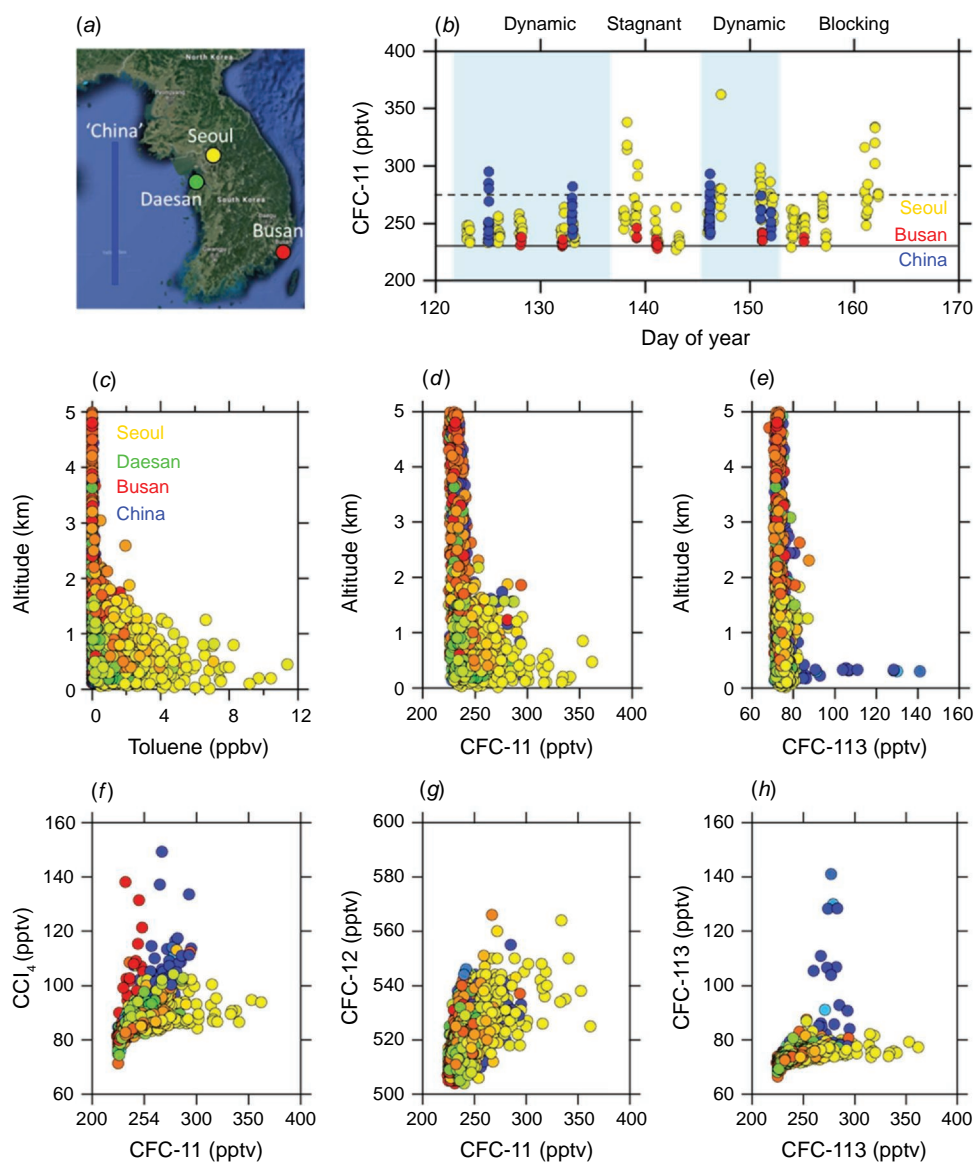


Fig. 11. CFC-11 mixing ratios measured over the Korean peninsula in spring, 2016 during KORUS-AQ. (a) Major sampling locations; (b) low-altitude (< 500 m) CFC-11 mixing ratios during dynamic (light blue shading) and stagnant (white) meteorological conditions for Seoul ($n = 177$), Busan ($n = 32$) and air arriving from China ($n = 66$); altitude vs (c) toluene (a tracer of air from Seoul), (d) CFC-11 and (e) CFC-113 (a tracer of air from China) ($n = 2554$); CFC-11 vs (f) CCl_4 , (g) CFC-12 and (h) CFC-113 ($n = 2554$). Mixing ratios are colour-coded by longitude: blue = China; green = Daesan (industry); yellow = Seoul; red = Busan.

362 pptv or $1.56 \times$ background (Table 2). These results are similar to those in 2015 during MAPS-Seoul (see above). Even though Seoul lies downwind of Shandong Province, where excess CFC-11 emissions were occurring in 2016 (Rigby *et al.* 2019), many of the elevated CFC-11 mixing ratios over Seoul were observed during stagnant rather than dynamic periods (Fig. 11c). Indeed, the average CFC-11 mixing ratio was higher during the two stagnant periods (260 ± 24 pptv) than during the two dynamic periods

(255 ± 21 pptv), though the difference is not statistically significant ($P = 0.24$) (Table 5). A total of 12% of Seoul samples were over background + 20% during KORUS-AQ, and 22% during MAPS-Seoul.

The regional pattern of CFC-11 enhancements was compared to other long-lived halocarbons measured during KORUS-AQ. In contrast to CFC-11, which was primarily enhanced over Seoul in northwest Korea (Fig. 11d), CCl_4 was primarily elevated over southeast Korea near Busan – consistent with regional inverse

modeling of CCl_4 emissions from Korea (Lunt *et al.* 2018) – and in air arriving from China (Fig. 11f). By comparison, CFC-113 and CFC-114 were only strongly elevated in air arriving from China (Fig. 11e; Simpson *et al.* 2020). In contrast to CFC-11 and other long-lived halocarbons, CFC-12 showed comparatively weak enhancements in air from both Seoul and China (Fig. 11g). Its average enhancement over background was 2% for both Seoul and China, with maximum enhancements of less than 10%. The altitude plot of CFC-11 more strongly resembled that of the Seoul tracer toluene than the other long-lived halocarbons (Fig. 11c–e). Overall, this indicates local CFC-11 emissions from the Seoul area during the spring 2016 timeframe, in a pattern that was different from other long-lived halocarbons.

Rough CFC-11 emissions for Seoul were based on a simple calculation using CO emissions from the KORUS-AQ v5.0 emission inventory (Woo *et al.* 2020). Unlike other halocarbons such as CFC-113 and CFC-114, CFC-11 showed some correlation with CO in Seoul during KORUS-AQ ($r^2 = 0.44$) and MAPS-Seoul ($r^2 = 0.79$) (Fig. 12). The KORUSv5 emission inventory estimates CO emissions of 90 Gg year^{-1} in Seoul and 390 Gg year^{-1} in greater Seoul during 2015. CFC-11 emissions were calculated using Eqn. 1, where in this case $\Delta\text{CFC11}/\Delta\text{CO}$ is the slope measured during MAPS-Seoul and KORUS-AQ (Fig. 12a, b). This simple calculation assumes that CFC-11 emissions can be determined based on CO emissions, that springtime measurements apply year-round and that 2015 CO emissions apply equally in both 2015 and 2016. Given these uncertainties, the calculation is only intended to determine a rough magnitude of CFC-11 emissions from Seoul relative to the global CFC-11 excess during the 2015–2016 timeframe. Bearing this in mind, CFC-11 emissions are estimated to be $0.06\text{--}0.10 \text{ Gg year}^{-1}$ in Seoul and $0.24\text{--}0.42 \text{ Gg year}^{-1}$ in greater Seoul during the 2015–2016 timeframe. This represents 0.6–4% of the 10 Gg year^{-1} of global CFC-11 excess in 2014–2016 compared to 2002–2012 (Engel and Rigby 2018), and 0.5–3% of the 13 Gg year^{-1} of excess CFC-11 in 2014–2018 compared

to 2008–2012 (Montzka *et al.* 2021). These values also represent 1–11% of the $4\text{--}5 \text{ Gg year}^{-1}$ that is attributed to non-China sources of CFC-11, assuming 40% of excess CFC-11 originated outside of eastern China (Park *et al.* 2021). New CFC-11 emission sources during this timeframe include newly produced CFC-11 usage in closed-cell foams (Technology and Economic Assessment Panel (TEAP) 2021). These estimates represent an upper limit because we are unable to determine what proportion of the CFC-11 emission estimates represent potential new emissions in 2014–2016 compared to existing emissions prior to the CFC-11 slow-down (as noted previously, post-phaseout emissions of CFC-11 are expected for many years from CFC-11 banks). Nonetheless, this analysis indicates ongoing CFC-11 emissions in the Seoul area during 2015–2016.

Rigby *et al.* (2019) and Park *et al.* (2021) used high-frequency CFC-11 measurements from Gosan, South Korea (about 500 km south of Seoul) to estimate CFC-11 emissions from East Asia. From 2014 to 2017, CFC-11 emissions from South Korea were small compared to Shandong and Hebei provinces, and CFC-11 emissions in Seoul were not elevated compared to the rest of South Korea. This may be because of less sensitivity of the Gosan station to Seoul compared to the KORUS-AQ data. Consistent with this, Lunt *et al.* (2018) reported emission estimates of CCl_4 in the same region using both Gosan data and KORUS-AQ data. A region of enhanced emissions in southeast Korea was more prominent in the KORUS-AQ data than the Gosan data, likely because of greater sensitivity of the KORUS-AQ data to this area (Lunt *et al.* 2018). 2b. Daesan (May–June, 2016). Average CFC-11 levels in low-altitude samples collected downwind of the Daesan petrochemical facility were $251 \pm 6 \text{ pptv}$, or $1.08 \times$ background, with a maximum of 260 pptv , or $1.12 \times$ background (Table 2). In addition to much lower maximum CFC-11 levels at Daesan vs Seoul (260 vs 362 pptv , respectively), the average Daesan value was lower than Seoul (Table 2; $P = 0.05$). The average wind direction during Daesan sampling was southwest (SW) on June 2, south-southwest (SSW) on June 3, and east-northeast (ENE) on June 5, 2016 (Fried *et al.* 2020).

Table 5. Statistics of selected VOCs measured at low altitude over Seoul during KORUS-AQ, during dynamic ($n = 78$) and stagnant ($n = 99$) meteorological conditions.

Meteorology	CFC-11 (pptv)	CFC-12 (pptv)	CFC-113 (pptv)	CCl_4 (pptv)	OCS (pptv)	1,2-DCE (pptv)	Toluene (ppbv)
Dynamic	255.4 ± 20.7	527.3 ± 7.7	75.3 ± 2.1	89.0 ± 5.6	751 ± 151	124 ± 99	1.77 ± 1.14
Stagnant	259.5 ± 24.4	528.2 ± 9.6	74.9 ± 1.8	86.7 ± 3.2	657 ± 112	91 ± 62	2.69 ± 2.15
P-value	$P = 0.24$	$P = 0.50$	$P = 0.17$	$P = 0.0007$	$P < 0.0001$	$P = 0.0074$	$P = 0.0008$

Carbonyl sulfide (OCS) and 1,2-dichloroethane (1,2-DCE) are examples of tracers of air from China during KORUS-AQ, and were more elevated during dynamic transport conditions; toluene is tracer for Seoul that, like CFC-11, was more elevated during stagnant conditions.

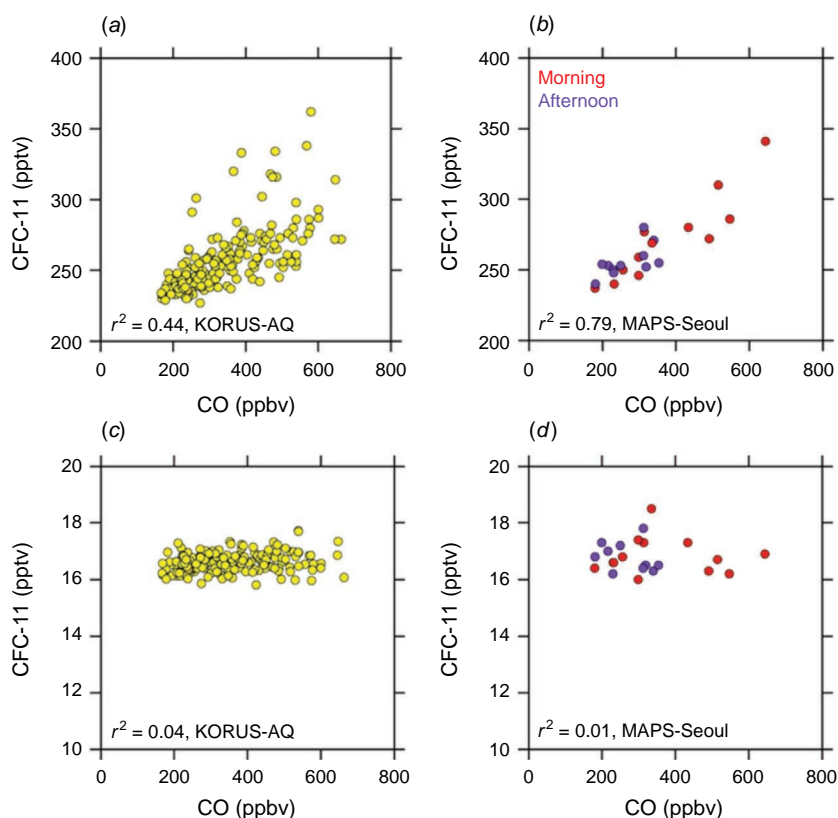


Fig. 12. Mixing ratios of CFC-11, CFC-114 and CO measured in Seoul during KORUS-AQ (2016) and MAPS-Seoul (2015). CFC-11 vs CO during (a) KORUS-AQ and (b) MAPS-Seoul; CFC-114 vs CO during (c) KORUS-AQ and (d) MAPS-Seoul.

The average CFC-11 mixing ratio did not differ under SWSSW and ENE wind directions (250.8 ± 7.0 pptv and 251.4 ± 4.3 pptv, respectively; $P = 0.75$), indicating that the Daesan CFC-11 levels were not impacted from Seoul (80 km to the NE).

2c. Busan (May–June, 2016), South Korea. Average CFC-11 levels in low-altitude samples near Busan in southeast Korea were 235 ± 4 pptv, or $1.01 \times$ background, with a maximum of 246 pptv or $1.06 \times$ background (Table 2). These values are much lower than those observed in Seoul or in air arriving from China (Fig. 11c), indicating relatively low CFC-11 emission in southeast Korea during the KORUS-AQ timeframe.

2d. Outflow from China. Air recently impacted from eastern China and sampled at low altitude over the Yellow Sea had a CFC-11 average of 254 ± 14 pptv or $1.10 \times$ background, and a maximum of 295 pptv or $1.27 \times$ background (Table 2). The average is higher than in Busan ($P < 0.0001$) and slightly lower than in Seoul ($P = 0.19$). Because CFC-11 levels were not higher in air arriving from China than in Seoul (Fig. 11c), China is not the primary source of elevated CFC-11 levels in Seoul, which appear to be local. The CFC-11 levels measured over the Yellow Sea during KORUS-AQ (2016) are within the range of the ground-based measurements in Shandong province (2014–2018), and more closely approximate the lower CFC-11 enhancements measured in Tuoji Island and

Qingdao than the higher inland values at Mount Tai and Dongying (Table 2).

Discussion

UCI has collected urban air samples in many regions of Asia since 1998. Although these studies were typically designed for other purposes, such as determining major ozone precursors, they also provide long-term records of CFC-11 over the period during which the Montreal Protocol took effect. Elevated CFC-11 levels in urban areas are expected for many years even in countries that are compliant with the Montreal Protocol, because of ongoing release from existing banks. For example, CFC-11 foam products that were produced before 2010 may not reach their end-of-life for another 20–50 years (Technology and Economic Assessment Panel (TEAP) 2021). However, CFC-11 enhancements that do not decrease much after phaseout may at least provide a guide for identifying potential unreported emissions. While the comparison of measurements from city to city can be impacted by factors such as proximity to local sources, boundary layer height and so forth, the measurements in each city were designed to minimise these effects as much as possible, with the overall goal of obtaining representative sampling in urban spaces away from immediate local source influences.

The first major outcome reported in this paper is the analysis of CFC-11 mixing ratios measured in cities

throughout Asia from 1998 to 2018, mainly in previously unstudied cities, and some new estimates of CFC-11 emissions. For instance, these studies provide the first CFC-11 measurements of which we are aware in Nepal, Pakistan and Saudi Arabia. While several pre-phaseout measurements in Karachi, Pakistan were greater than background +20%, almost all urban post-phaseout measurements in Pakistan (Lahore), Saudi Arabia (Mecca, Medina, Jeddah) and Nepal (Kathmandu, Bode) were within background +20%. This suggests that unreported CFC-11 emissions in these regions are less likely. The studies reported here also provide valuable ground-based measurements in other areas of interest, including China and South Korea, both before (in the case of China) and during the timeframe in which global CFC-11 levels were declining more slowly than expected. While pre-phaseout CFC-11 mixing ratios in many cities in China were within background +20%, average values in Jinan, Hangzhou and Beijing were greater than this threshold. After the 2010 phaseout, average CFC-11 values were still greater than background +20% in an inland area of Shandong Province, consistent with the literature and suggesting elevated CFC-11 emissions. Excess CFC-11 levels also stood out in Seoul and were consistent with locally emitted CFC-11 as opposed to transboundary transport. Translating the urban CFC-11 mixing ratios to emissions is subject to a number of limitations and uncertainties. In this work, CFC-11 emissions of 0.2–0.4 Gg year⁻¹ were estimated for the greater Seoul region in 2015 and 2016. These values are within the range of emission estimates reported for South Korea in this timeframe by Rigby et al. (2019), and South Korea does not appear to be a major global source of unreported CFC-11 despite the elevated CFC-11 values.

The second major finding from this work is the presence of local sources of CFC-11 from garbage burning and landfill fires in Asia. Based on limited measurements of excess CFC-11 from garbage fires in Nepal and a landfill fire in Mecca, Saudi Arabia, global CFC-11 estimates on the order of 1–4 Gg year⁻¹ were estimated from garbage burning. Because of the limited measurements of CFC-11 from garbage burning, it was not possible to determine whether some regions have relatively stronger CFC-11 emissions from garbage burning sources, or how CFC-11 emissions from garbage burning may have changed over time. It also was not possible to determine whether garbage burning sources may have influenced the less negative CFC-11 trends detected by AIRS in these regions from 2013–2018 (Chen et al. 2000), and more comprehensive sampling in the Arabian Peninsula and Nepal is recommended.

Conclusions

CFC-11 levels were measured in urban areas of Asia from 1998 to 2018, including pre-phaseout studies in China and Pakistan, and post-phaseout studies in China, Nepal, Pakistan,

Saudi Arabia and South Korea. The post-phaseout measurements overlapped the 2012–2018 period in which global CFC-11 emissions declined less slowly than expected, primarily because of increased emissions from Asia. Prior to the 2010 phaseout, higher CFC-11 levels were measured in China than in Pakistan (up to 6.0× background in Beijing versus 2.3× in Karachi), even though overall VOC levels were much higher in Karachi. Maximum CFC-11 levels were lower after the 2010 phaseout, and were larger in Shandong Province, China (up to 1.7× background), Seoul, South Korea (1.6×) and Jeddah, Saudi Arabia (1.6×) than in urban areas of Mecca, Saudi Arabia (1.1×), Lahore, Pakistan (1.2×) and Kathmandu, Nepal (1.3×), although we bear in mind the small sample size for some of the post-phaseout studies. In contrast to almost all post-phaseout urban CFC-11 measurements in Nepal, Pakistan and Saudi Arabia, many CFC-11 samples in Seoul and in air arriving from China were greater than background +20%, showing ongoing emissions in these regions during the 2014–2018 timeframe. Rough calculations suggest that the Korean CFC-11 emissions may represent up to 1–11% of excess CFC-11 emissions originating outside of East Asia. Roadside garbage burning in Nepal and a landfill fire in Saudi Arabia were notable CFC-11 sources, with maximum CFC-11 levels of 2.7–2.8× background. Rough emission estimates indicate that open burning of garbage and landfills could potentially emit 1–4 Gg year⁻¹ of CFC-11 globally. However, further study of garbage burning sources is encouraged in order to determine a robust emission estimate, especially as global CFC-11 levels continue to decline and smaller sources become increasingly important (Wang et al. 2021). Overall, these measurements provide important observational constraints on recent CFC-11 emission regions in Asia, including understudied source signatures (e.g. garbage burning, landfill fires) and undersampled countries in Asia.

References

- Anjum M, Miandad R, Waqas M, Ahmad I, Alafif ZOA, Aburizaiza AS, Barakat MA, Akhtar T (2016) Solid waste management in Saudi Arabia: a review. *Journal of Applied Agriculture and Biotechnology* 1(1), 13–26.
- Barletta B, Meinardi S, Simpson IJ, Khwaja HA, Blake DR, Rowland FS (2002) Mixing ratios of volatile organic compounds (VOCs) in the atmosphere of Karachi, Pakistan. *Atmospheric Environment* 36, 3429–3443. doi:10.1016/S1352-2310(02)00302-3
- Barletta B, Meinardi S, Simpson IJ, Rowland FS, Chan C-Y, et al. (2006) Ambient halocarbon mixing ratios in 45 Chinese cities. *Atmospheric Environment* 40, 7706–7719. doi:10.1016/j.atmosenv.2006.08.039
- Barletta B, Simpson IJ, Blake NJ, Meinardi S, Emmons LK, et al. (2017) Characterization of carbon monoxide, methane and nonmethane hydrocarbons in emerging cities of Saudi Arabia and Pakistan and in Singapore. *Journal of Atmospheric Chemistry* 74, 87–113. doi:10.1007/s10874-016-9343-7
- Benish SE, Salawitch RJ, Ren X, He H, Dickerson RR (2021) Airborne Observations of CFCs Over Hebei Province, China in Spring 2016. *Journal of Geophysical Research: Atmospheres* 126(18), doi:10.1029/2021jd035152
- Blake DR, Rowland FS (1995) Urban leakage of liquefied petroleum gas and its impact on Mexico City air quality. *Science* 269(5226), 953–956. doi:10.1126/science.269.5226.953
- Carpenter LJ, Reimann S (Lead Authors), Burkholder JB, Clerbaux C, Hall BD, Hossaini R, Laube JC, Yvon-Lewis SA (2014) Chapter 1: Update

- on ozone-depleting substances (ODSs) and other gases of interest to the Montreal Protocol. In 'Scientific Assessment of Ozone Depletion: 2014, Global Ozone Research and Monitoring Project – Report No. 55'. (World Meteorological Organization, Geneva, Switzerland)
- Chen X, Huang X, Strow LL (2020) Near-global CFC-11 trends as observed by atmospheric infrared sounder from 2003 to 2018. *Journal of Geophysical Research* **125**, 22. doi:10.1029/2020JD033051
- Colman JJ, Swanson AL, Meinardi S, Sive BC, Blake DR, Rowland FS (2001) Description of the analysis of a wide range of volatile organic compounds in whole air samples collected during PEM-Tropics A and B. *Analytical Chemistry* **73**, 3723–3731. doi:10.1021/ac010027
- Crawford JH, Ahn J-Y, Al-Saadi J, Chang L, Emmons LK, Kim J, et al. (2021) The Korea-United States Air Quality (KORUS-AQ) field Study. *Elementa: Science of the Anthropocene* **9**(1), 1–27. doi:10.1525/elementa.2020.00163
- Engel A, Rigby M (Lead Authors), Burkholder JB, Fernandez RP, Froidevaux L, Hall BD, Hossaini R, Saito T, Vollmer MK, Yao B (2018) Chapter 1: Update on ozone-depleting substances (ODSs) and other gases of interest to the Montreal Protocol. In 'Scientific Assessment of Ozone Depletion: 2018, Global Ozone Research and Monitoring Project – Report No. 58'. (World Meteorological Organization, Geneva, Switzerland)
- Fraser PJ, Dunse BL, Krummel PB, Steele LP, Derek N (2020) Australian chlorofluorocarbon (CFC) emissions: 1960–2017. *Environmental Chemistry* **17**, 525–544. doi:10.1071/EN19322
- Fried A, Walega J, Weibring P, Richter D, Simpson IJ, et al. (2020) Airborne formaldehyde and VOC measurements over the Daesan Petrochemical Complex on Korea's northwest coast during the KORUS-AQ Study: estimation of emission fluxes and potential effects on air quality. *Elementa: Science of the Anthropocene* **8**, 1. doi:10.1525/elementa.2020.121
- Gilpin TM (1991) Global concentrations of three chlorofluorocarbons, 1984–1988. PhD dissertation, University of California, Irvine.
- Goetz JD, Giordano MR, Stockwell CE, Christian TJ, Adhikari R, Bhawe PV, Praveen PS, Panday AK, Jayarathne T, Stone EA, Yokelson RJ, DeCarlo PF (2018) Speciated online PM₁ from South Asian combustion sources – Part 1: fuel-based emission factors and size distributions. *Atmospheric Chemistry and Physics* **18**, 14653–14679. doi:10.5194/acp-18-14653-2018
- Gullett BK, Wyrzykowska B, Grandesso E, Touati A, Tabor DG, Solórzano Ochoa G (2010) PCDD/F, PBDD/F, and PBDE emissions from open burning of a residential waste dump. *Environmental Science & Technology* **44**, 394–399. doi:10.1021/es902676w2010
- Hall BD, Engel A, Mühle J, Elkins JW, Artuso F, et al. (2014) Results from the International Halocarbons in Air Comparison Experiment (IHALACE). *Atmospheric Measurement Techniques* **7**, 469–490. doi:10.5194/atm-7-469-2014
- Harris NRP, Montzka SA, Newman PA, et al. (2019) Report on the international symposium on the unexpected increase in emissions of ozone-depleting CFC-11, Stratosphere-troposphere Processes and their Role in Climate (SPARC), Newsletter no. 53, July 2019.
- Hegg DA, Radke LF, Hobbs PV, Rasmussen RA, Riggan PJ (1990) Emissions of some trace gases from biomass fires. *Journal of Geophysical Research* **95**(D5), 5669–5675.
- Hodson EL, Martin D, Prinn RG (2010) The municipal solid waste landfill as a source of ozone-depleting substances in the United States and United Kingdom. *Atmospheric Chemistry and Physics* **10**, 1899–1910. doi:10.5194/acp-10-1899-2010
- Islam Md R, Jayarathne T, Simpson IJ, Werden B, Maben J, et al. (2020) Ambient air quality in the Kathmandu Valley, Nepal during the pre-monsoon: concentrations and sources of particulate matter and trace gases. *Atmospheric Chemistry and Physics* **20**, 2927–2951. doi:10.5194/acp-20-2927-2020
- Kim H, Choi W-C, Rhee H-J, Suh I, Lee M, et al. (2018a) Meteorological and chemical factors controlling ozone formation in Seoul during MAPS-Seoul 2015. *Aerosol and Air Quality Research* **18**, 2274–2286. doi:10.4209/aaqr.2017.11.0445
- Kim S, Jeong D, Sanchez D, Wang M, Seco R, et al. (2018b) The controlling factors of photochemical ozone production in Seoul, South Korea. *Aerosol and Air Quality Research* **18**, 2253–2261. doi:10.4209/aaqr.2017.11.0452
- Kumar A, Sinha V, Shabin M, Hakkim H, Bonsang B, Gros V (2020) Non-methane hydrocarbon (NMHC) fingerprints of major urban and agricultural emission sources for use in source apportionment studies. *Atmospheric Chemistry and Physics* **20**, 12133–12152. doi:10.5194/acp-20-12133-2020
- Lickley M, Solomon S, Fletcher S, Velders GJM, Daniel J, Rigby M, Montzka SA, Kuijpers LJM, Stone K (2020) Quantifying contributions of chlorofluorocarbon banks to emissions and impacts on the ozone layer and climate. *Nature Communications* **11**, 1380. doi:10.1038/s41467-020-15162-7
- Lin Y, Gong D, Lv S, Ding Y, Wu G, et al. (2019) Observations of high levels of ozone-depleting CFC-11 at a remote mountain-top site in Southern China. *Environmental Science & Technology Letters* **6**, 114–118. doi:10.1021/acs.estlett.9b00022
- Lunt MF, Park S, Li S, Henne S, Manning AJ, et al. (2018) Continued emissions of the ozone-depleting substance carbon tetrachloride from Eastern Asia. *Geophysical Research Letters* **45**, 11423–11430. doi:10.1029/2018GL079500
- Montzka SA, Dutton GS, Yu P, Ray E, Portmann RW, et al. (2018) An unexpected and persistent increase in global emissions of ozone-depleting CFC-11. *Nature* **557**, 413–417. doi:10.1038/s41586-018-0106-2
- Montzka SA, Dutton GS, Portmann RW, Chipperfield MP, Davis S, et al. (2021) A decline in global CFC-11 emissions during 2018–2019. *Nature* **590**, 428–432. doi:10.1038/s41586-021-03260-5
- Park S, Western LM, Saito T, Redington AL, Henne S, et al. (2021) A decline in emissions of CFC-11 and related chemicals from eastern China. *Nature* **590**, 433–437. doi:10.1038/s41586-021-03277-w
- Peterson DA, Hyer EJ, Han S-O, Crawford JH, Park RJ, et al. (2019) Meteorology influencing springtime air quality, pollution transport, and visibility in Korea. *Elementa: Science of the Anthropocene* **7**, 57. doi:10.1525/elementa.395
- Rigby M, Park S, Saito T, Western LM, Redington AL, et al. (2019) Increase in CFC-11 emissions from eastern China based on atmospheric observations. *Nature* **569**, 546–550. doi:10.1038/s41586-019-1193-4
- Scheutz C, Dote Y, Fredenslund AM, Mosbæk H, Kjeldsen P (2007) Attenuation of fluorocarbons released from foam insulation in landfills. *Environmental Science & Technology* **41**, 7714–7722. doi:10.1021/es0707409
- Simpson IJ, Akagi SK, Barletta B, Blake NJ, Choi Y, et al. (2011) Boreal forest fire emissions in fresh Canadian smoke plumes: C₁-C₁₀ volatile organic compounds (VOCs), CO₂, CO, NO₂, NO, HCN and CH₃CN. *Atmospheric Chemistry and Physics* **11**, 6445–6463. doi:10.5194/acp-11-6445-2011
- Simpson IJ, Sulbaek Andersen MP, Meinardi S, Bruhwiler L, Blake NJ, Helmig D, Rowland FS, Blake DR (2012) Long-term decline of global atmospheric ethane concentrations and implications for methane. *Nature* **488**(7412), 490–494. doi:10.1038/nature11342
- Simpson IJ, Aburizaiza OS, Siddique A, Barletta B, Blake NJ, et al. (2014) Air quality in Mecca and surrounding holy places in Saudi Arabia during Hajj: Initial survey. *Environmental Science & Technology* **48**, 8529–8539. doi:10.1021/es5017476
- Simpson IJ, Blake DR, Blake NJ, Meinardi S, Barletta B, et al. (2020) Characterization, sources and reactivity of volatile organic compounds (VOCs) in Seoul and surrounding regions during KORUS-AQ. *Elementa: Science of the Anthropocene* **8**, 37. doi:10.1525/elementa.434
- Stockwell CE, Christian TJ, Goetz JD, Jayarathne T, Bhawe PV, et al. (2016) Nepal Ambient Monitoring and Source Testing Experiment (NAMASte): emissions of trace gases and light-absorbing carbon from wood and dung cooking fires, garbage and crop residue burning, brick kilns, and other sources. *Atmospheric Chemistry and Physics* **16**, 11043–11081. doi:10.5194/acp-16-11043-2016
- Technology and Economic Assessment Panel (TEAP) (2021) TEAP Report, May 2021, Volume 3: Decision XXXI/3 TEAP Task Force Report on Unexpected Emissions of Trichlorofluoromethane (CFC-11), Montreal Protocol on Substances that Deplete the Ozone Layer, United Nations Environment Programme (UNEP).
- Tyler SC (1983) Chlorinated hydrocarbons in the troposphere. PhD dissertation, University of California, Irvine.
- Ul-Haq Z, Ali M, Batool SA, Tariq S, Qayyum Z (2016) Emission quantification of refrigerant CFCs, HCFCs and HFCs in megacity Lahore (Pakistan) and contributed ODPs and GWPs. *Journal of Earth System Science* **125**(6), 1273–1284. doi:10.1007/s12040-016-0724-8
- US Fire Administration(2001) Landfill fires. *Topical Fire Research Series* **1**(18), 1–5.

- Wang T, Nie W, Gao J, Xue LK, Gao XM, et al. (2010) Air quality during the 2008 Beijing Olympics: secondary pollutants and regional impact. *Atmospheric Chemistry and Physics* **10**, 7603–7615. doi:10.5194/acp-10-7603-2010
- Wang P, Scott JR, Solomon S, Marshall J, Babbin AR, Lickley M, Thompson DWJ, deVries T, Liang Q, Prinn RG (2021) On the effects of the ocean on atmospheric CFC-11 lifetimes and emissions. *Proceedings of the National Academy of Sciences of the United States of America* **118**(12), e2021528118. doi:10.1073/pnas.2021528118
- Warner J, Wei Z, Strow L, Barnet CD, Sparling LC, Diskin GS, Sachse G (2010) Improved agreement of AIRS tropospheric carbon monoxide products with other EOS sensors using optimal estimation retrievals. *Atmospheric Chemistry and Physics* **10**, 9521–9533. doi:10.5194/acp-10-9521-2010
- Wiedinmyer C, Yokelson RJ, Gullett BK (2014) Global emissions of trace gases, particulate matter, and hazardous air pollutants from open burning of domestic waste. *Environmental Science & Technology* **48**, 9523–9530. doi:10.1021/es502250z
- Woo J-H, Kim Y, Kim H-K, Choi K-C, Eum J-H, Lee J-B, Lim J-H, Kim J, Seong M (2020) Development of the CREATE inventory in support of integrated climate and air quality modeling for Asia. *Sustainability* **12**(19), 7930. doi:10.3390/su12197930
- Yi L, Wu J, An M, Xu W, Fang X, Yao B, Li Y, Gao D, Zhao X, Hu J (2021) The atmospheric concentrations and emissions of major halocarbons in China during 2009–2019. *Environmental Pollution* **284**, 117190. doi:10.1016/j.envpol.2021.117190
- Zhang F, Chen Y, Tian C, Wang X, Huang G, et al. (2014) Identification and quantification of shipping emissions in Bohai Rim, China. *Science of the Total Environment* **497–498**, 570–577. doi:10.1016/j.scitotenv.2014.08.016
- Zhao F, Chen T-S, Dong C, Li H-Y, Liu Z, Bi Y-J, Guo Z-X, Wang X-F, Wang T, Wang W-X, Xue L-K (2022) Long-term trend and sources of atmospheric halocarbons at Mount Taishan, Northern China. *Environmental Science* **43**(2), 723–734. [In Chinese] doi:10.13227/j.hjxx.202103231
- Zheng P, Chen T, Dong C, Liu Y, Li H, Han G, Sun J, Wu L, Gao X, Wang X, Qi Y, Zhang Q, Wang W, Xue L (2019) Characteristics and sources of halogenated hydrocarbons in the Yellow River Delta region, northern China. *Atmospheric Research* **225**, 70–80. doi:10.1016/j.atmosres.2019.03.039

Data availability. The KORUS-AQ data are available at <https://www-air.larc.nasa.gov/cgi-bin/ArcView/korusaq>. The remaining data that support this study will be shared upon reasonable request to the corresponding author.

Conflicts of interest. Elizabeth Stone is an Editor of *Environmental Chemistry* but was blinded from the peer-review process for this paper. The authors declare no other conflicts of interest.

Declaration of funding. The authors thank the many agencies that have funded the projects presented in this paper. The 45-city study in China was funded by the Research Grants Council of Hong Kong (RGC). The Beijing Olympics study was funded by RGC, the National Basic Research Program of China, and the Hong Kong Polytechnic University (HKPU). The Pakistan studies were funded by the United Nations Development Program (UNDP) and the National Talent Pool of the Government of Pakistan. The Saudi Arabia studies were funded by the King Abdulaziz University in Jeddah. The Nepal study was funded by the National Science Foundation (NSF) and the International Centre for Integrated Mountain Development (ICIMOD), with additional support from NSF grant AGS-1351616 (EA Stone). KORUS-AQ was funded by the National Aeronautics and Space Administration (NASA) and the National Institute of Environmental Research (NIER). UCI's long-term background air sampling in the Pacific Basin is funded by NASA (grant NNX16AK04G). The authors also thank the Gary Comer Abrupt Climate Change Fellowship for support.

Acknowledgements. The authors thank the many people who collected and analysed the UCI air samples from 1998 to 2018, and the teams that supported the projects and missions over these years. They especially thank UCI group members Barbara Chisholm, Brent Love and Gloria Liu Weitz. They gratefully acknowledge Glenn Diskin and team for DACOM CO data used in the KORUS-AQ analysis, and Alan Fried for wind direction analysis during KORUS-AQ. The authors acknowledge the NOAA Air Resources Laboratory (ARL) for providing access to the HYSPLIT transport and dispersion model. They thank the UC White Mountain Research Center for supporting the use of the Crooked Creek Station to collect air samples for use as working standards. The authors also thank three reviewers for their constructive comments on the manuscript.

Author affiliations

^ADepartment of Chemistry, University of California–Irvine (UCI), Irvine, CA, USA.

^BUniversity for Ain Zubaida Rehabilitation and Groundwater Research, King Abdulaziz University, Jeddah, Saudi Arabia.

^CDepartment of Environmental Health and Engineering, Johns Hopkins University, Baltimore, MD, USA.

^DDepartment of Chemistry, Forman Christian College (A Chartered University), Lahore, Pakistan.

^EDepartment of Environmental Health Sciences, School of Public Health, University at Albany, Albany, NY, USA.

^FWadsworth Center, New York State Department of Health, Albany, NY, USA.

^GDepartment of Advanced Technology Fusion, Konkuk University, Seoul, South Korea.

^HInternational Institute for Applied Systems Analysis, Laxenburg, Austria.

^IUllens Education Foundation, Lalitpur, Nepal.

^JInstitute for Integrated Development Studies, Kathmandu, Nepal.

^KEnvironment and Sustainability Center, QEERI, Hamad Bin Khalifa University, Doha, Qatar.

^LDepartment of Chemistry, University of Iowa, Iowa City, IA, USA.

^MDepartment of Civil and Environmental Engineering, The Hong Kong Polytechnic University, Hong Kong, China.

^NEnvironment Research Institute, Shandong University, Jinan, Shandong, China.

^ODepartment of Chemistry, University of Montana, Missoula, MT, USA.

^PDepartment of Environment and Health Research, The Custodian of the Two Holy Mosques Institute for Hajj and Umrah Research, Umm al Qura University, Mecca, Saudi Arabia.